EXTRACTING FUZZY RULES TO COMPARE GENETIC ALGORITHM-GENERATED MOTONEURON MODELS

by

ERIC WILT

A THESIS

Submitted to the faculty of Delaware State University in partial fulfillment of the requirements for the degree of Master of Science in Computer Science in the Division of Physical and Computational Sciences

DOVER, DELAWARE
May 2019

This thesis is approved by the following members of the Final Oral Review Committee:

Dr. Tomasz Smolinski, Committee Chairperson, Division of Physical and Computational Sciences, Delaware State University

Dr. Kam Kong, Committee Member, Division of Physical and Computational Sciences, Delaware State University

Dr. Fatima Boukari, Committee Member, Division of Physical and Computational Sciences, Delaware State University

Dr. Melissa Harrington, External Committee Member, Professor of Biology, Delaware State University

DEDICATION

This thesis is dedicated to my wife, Kimberly, and our children, Emma and Maximilian, without whose support, love, consideration, understanding, and sacrifice, none of my graduate work would have been possible. My deepest gratitude, appreciation, and love are with them, always.

ACKNOWLEDGEMENTS

There are a number of people who deserve my most sincere thanks:

Dr. Tomasz Smolinski, for agreeing to take on the role of chairperson for my thesis committee. Without his guidance, support, and expertise, this thesis would have been largely directionless.

Dr. Melissa Harrington's support was instrumental in keeping me tied to this project. I am honored that she accepted the invitation to be the external member of my thesis committee.

Dr. Gary Holness, for his excellence and professionalism in the roles of teacher and graduate program director.

Drs. Kam Kong and Fatima Boukari, in whose classrooms I thoroughly enjoyed being and who graciously accepted positions on my thesis committee.

Dr. Marwan Rasamny, for his exceptional leadership as Chairperson of the Division of Physical and Computational Sciences.

Dr. Venu Kalavacharla, who, through his Center for Integrated Biological & Environmental Research (CIBER), generously supported my earlier graduate work.

This material is based upon work supported by the National Science Foundation under Grant No. 1608147.

Any opinions, findings, and conclusions or recommendations expressed in this material are those of the author and do not necessarily reflect the views of the National Science Foundation.

Extracting Fuzzy Rules to Compare Genetic Algorithm-Generated Motoneuron Models

Eric Wilt

Faculty Advisor: Dr. Tomasz Smolinski

ABSTRACT

Spinal motoneurons that have been active for prolonged periods of time exhibit different electrical properties than their less active counterparts, suggesting that prolonged neuronal activity may change how electrical signals are transmitted through the neuron. Understanding how these spinal motoneurons integrate their input signals and modulate their output is important, with implications for rehabilitation, advanced prosthetics, brain-machine interfaces, humanoid robotics, and other biologically-inspired systems.

To investigate what changes may take place within a spinal motoneuron following prolonged activity, a genetic algorithm was employed to generate two distinct groups of spinal motoneuron computational models. The first group (control) simulated less active neurons while the second group simulated neurons treated with high K^+, which mimics persistent activation. The models had nine variable parameters, each a conductance related to a specific ion channel present in the motoneuron. To evaluate fitness for each computational model, fuzzy logic was used to assign membership in fuzzy sets corresponding to two separate objectives: current threshold and input resistance. To mine rules from the generated data, correlations were looked at between each fuzzy set and each parameter.

While no rules were successfully mined in this research, some interesting results were produced. Some relationships that exist between parameters within the control (less active) models, do not seem to exist in the treated models. Relationships were also found between parameters that exist in both groups of models, suggesting a possible co-regulation of the genes which express those traits.

TABLE OF CONTENTS

LIST OF TABLES

LIST OF FIGURES

CHAPTER 1: INTRODUCTION

SECTION 1.1: BACKGROUND AND PROBLEM STATEMENT

Spinal motoneurons have a soma (cell body) that originates in the spinal cord and an axon that extends to provide motor control to some muscle or other organ in the body. Motoneurons that have been active for prolonged periods of time exhibit different electrical properties than their less active counterparts, suggesting that prolonged neuronal activity may change how electrical signals are transmitted through the neuron. Understanding how these spinal motoneurons integrate their input signals and modulate their output is important, with implications for rehabilitation, advanced prosthetics, brain-machine interfaces, humanoid robotics, and other biologically-inspired systems [1]. This work sought to investigate what changes may take place within a spinal motoneuron following prolonged activity.

Computational modeling of motoneuron activity can provide a bridge between the theoretical and experimental aspects of neuroscience. It can help alleviate the issue of requiring excessive quantities of organic laboratory samples while providing a way to perform reproducible, simplified experiments. Challenges lie in deciding how to model neurons in a way that is both meaningful to the investigation and also simple. Another challenge lies in tackling what happens when multiple objectives need to be optimized in order to determine how well a model performs overall.

Expanding on ideas in the thesis work of Parth Patel [2], this thesis combined computational modeling with techniques from the field of computational intelligence, namely genetic algorithms [3] and fuzzy logic [4]. Computational models were generated by a genetic algorithm and evaluated according to membership in fuzzy sets for the purpose of mining rules from the sets of created models.

Since this work was concerned with the changes that take place in motoneurons after experiencing prolonged activation, two experimental groups were needed. The first group was a control

group of computational models representing less active motoneurons. The second group was a group of computational models representing treated neurons. Laboratory study has shown that treatment with high K^+ (potassium ion) is likely to simulate sustained motor activity [1]. The treated neurons showed changes in electrical properties. The changes specifically important to this thesis work were reduced input resistance and increased threshold current, as summarized in Figure 2 of [1]. These two properties, threshold current and input resistance, were the objectives by which the computational models were evaluated.

SECTION 1.2: PURPOSE

One goal of this work was to create two separate databases of rules, one which applies to models representing less active spinal motoneurons and one which applies to models representing neurons treated with high K^+ (simulating prolonged activity). Contrasting these two rule sets was intended to provide insight as to what mechanisms are being changed by prolonged activation and how those mechanisms are changed. An extension of this goal would have been to apply the mined rules to the system creating the computational models, using fuzzy control, to see if the application of those rules provided better efficiency in generating good models.

Another goal was to see whether the rules generated change throughout the evolutionary process, probing in which generation might a certain rule appear or disappear and why that might have been the case.

This thesis was intended, in part, to have shed light on the relationship between the rules that were generated and the parameter search space, looking at whether certain rules only appeared (or never appeared) in certain areas of the search space. If such relationships existed, then reasons for those relationships might have been inferred.

Importantly, this work also sought biological relationships between various intrinsic properties of the motoneurons that the computational models represent. Specifically, this thesis examined the relationships that may exist between the conductances of different ion channels represented by the

parameters of the computational models.

SECTION 1.3: OVERVIEW

Computational models of spinal motoneurons were generated using a Multi-Objective Genetic Algorithm (MOGA). Use of a MOGA was deemed appropriate because of its specialization in exploring a search space to find optimal solutions and maintaining a diverse set of potential solutions while optimizing for multiple objectives. Models were generated in batches simulating both untreated motoneurons (as a control group) and treated motoneurons (treated with high K^+ to mimic persistent activation). Each model was simulated using the Neuron simulation environment [5]. Results of the simulations provided the data used to evaluate the models using fuzzy sets. Correlations were drawn between each batch's fuzzy sets and the parameters of the computational models to see if fuzzy rules could be mined. Correlations were also drawn between each parameter of the computational model and every other parameter to investigate biological relationships of the conductances of the ion channels that each of the parameters represent. The research design and method are detailed in Chapter 3.

SECTION 1.4: HYPOTHESIS

Pilot testing in small batches has shown that it is possible to extract fuzzy rules using the method proposed. An example of a rule discovered in pilot testing is shown in Chapter 3. The prediction going into this thesis was that the batches of motoneuron models would also produce rules. If rules could be produced for both the control group and the treated group, those rule sets could be compared as part of an exploration into how persistent activation affects spinal motoneurons. It was also expected that, by looking at how rules change throughout the evolutionary process of the genetic algorithm, patterns may appear.

SECTION 1.5: IMPORTANCE

This thesis work is significant in that it shows a successful application of a genetic algorithm to generate computational models of spinal motoneurons as well as the application of fuzzy logic to evaluate those models for fitness. It also provides a framework for the potential extraction of fuzzy rules based on correlations between objective fuzzy sets and parameters. This thesis also explores the relationships between the model parameters, which could potentially reveal evidence of co-regulation of the genes which express the traits that those parameters represent. Findings of this research are detailed in Chapter 4 and conclusions are discussed in Chapter 5.

SECTION 1.6: SCOPE AND LIMITATIONS

The models generated represent motoneurons; as such, the information learned in this research may not be applicable to other types of neurons.

The research itself was limited largely by time and computing resources. The simulation and analysis of each model is expensive in terms of computation time. A single batch of the size used in this research could take anywhere from two to five days to complete, depending on the resources of the machine running the simulations. Even with multiple machines running batches simultaneously, turnaround time is not ideal for very large production runs. Due to these time and resource constraints, this research could have benefitted from more generated models to increase the diversity of the samples.

CHAPTER 2: REVIEW OF LITERATURE

The models used in this work have their basis in a model originally developed by Alan Hodgkin and Andrew Huxley [6], [7], [8], [9], [10]. Hodgkin and Huxley performed experiments on the axon of a giant squid to develop a conductance-based model of how action potentials are generated and propagated in neurons. The Hodgkin-Huxley model represents the cell membrane as a capacitance, ion channels as conductances, gradients of electrochemical potential as voltage sources, and ion pumps as current sources. Hodgkin and Huxley used several differential equations to describe the properties and states associated with the model. Each computational model generated and used in this thesis has these basic components and is used as described by Hodgkin and Huxley.

Studies have been done, which used organic neuronal samples, that investigated factors that can change the intrinsic electrical properties of neurons. Jonathan Carp, Xiang-Yang Chen, Hesham Sheikh, and Jonathan Wolpaw studied how operant conditioning affects axonal conduction velocity and excitability in rat and primate motoneurons [11], [12]. They discovered that the spinal stretch reflex can be operantly conditioned and that such training changes axonal conduction velocity and excitability in motoneurons. Similarly, in other studies done on rat motoneurons, [13], [14], and [15] reveal that either exercise training or inactivity pull the electrical properties of motoneurons in opposite directions. This type of research is closely related to this thesis' investigation into how persistent activation changes the intrinsic electrical properties of motoneurons. The work of this thesis has the potential to add to the body of research of modeling changes in neuronal activity, specifically changes in electrical properties.

Computational models have been used to study motoneurons in the past. Gwendal Le Masson, Serge Przedborski, and L. F. Abbott used models built for the Neuron simulation environment [5] to study the degeneration of motoneurons [16]. Their research has implications in the study of amyotrophic lateral sclerosis (ALS). ALS patients experience a loss of motoneurons, which can

lead to muscle wasting and weakness. The work presented in [16] opens an important avenue of research to explore the link between certain neuronal processes and ALS.

The work in this thesis follows, in some ways, as an extension of the work done by Parth Patel in his 2013 Master's Thesis [2]. In his work, Patel explored using a hybrid of multi-objective evolutionary algorithm and fuzzy control system to generate and evaluate computational models of neurons. His intention was to provide the evolutionary algorithm with the ability to generate neuronal models with some expert biological knowledge. That knowledge came in the form of fuzzy IF-THEN rules applied through a fuzzy controller.

This thesis work attempts to mimic some of the successful aspects of Patel's work. First, Patel used the elitist, non-dominated vector-evaluated genetic algorithm (end-VEGA) [17] as the specific flavor of multi-objective evolutionary algorithm. The choice of this algorithm is important, as it is not the most computationally efficient option available; however, it does attempt to address some concerns about generating a diverse population of fit individuals. The elitist and non-dominating aspects try to ensure, via an archive, that the most fit individuals have a high probability of being perpetuated into successive generations of the evolutionary process.

Patel also used Pearson correlations between his established fuzzy sets and the parameters of his neuronal models to mine fuzzy rules. One of the main ideas of Patel's thesis was to use the mined rules in a fuzzy controller which worked in concert with the genetic algorithm to produce computational neuronal models with better overall fitness. It was one of the original intentions of this thesis work to include a component of fuzzy control, but a lack of rule generation and implementation issues precluded that from happening. Importantly, a methodology for attempting to mine rules from generated motoneuron models that was like Patel's was used in this thesis work.

Another major influence was the work of Joseph Lombardo, Jianli Sun, and Melissa Harrington [18], whose work directly follows from a proposal by Melissa Harrington and Tomasz Smolinski [1]. The work of these researchers provided the science which formed the theoretical framework on which this thesis is based. They employed the use of high K^+ treatment (to mimic persistent

activation) on real spinal motoneuron samples in a laboratory environment to explore the differences in less active motoneurons and persistently activated motoneurons. These authors provided empirical evidence that motoneurons experience an increase in the threshold current which induces an action potential and a decrease in input resistance following persistent activation. It is this work that inspired the question as to what changes are being made to the intrinsic electrical properties of spinal motoneurons after a period of prolonged activity. This is the question that lies at the heart of the explorations being made in this thesis.

CHAPTER 3: RESEARCH METHODS

SECTION 3.1: COMPUTATIONAL MODELS

The model that served as the basis for all generated models was crafted by students led by Dr. Tomasz Smolinski. The model is a combination of two previous models: a model of a Neocortex V1 L6 pyramidal corticothalamic cell, implemented by Maarten Kole (ModelDB Accession: 114394; https://senselab.med.yale.edu/ModelDB) [20] and spinal motoneuron model ok_m139 (NeuroMorpho.Org ID: NMO_00914) [21], [22], [23]. For this thesis, the axon and ion channels present in the Kole model were combined with the soma and dendritic structure of ok_m139. A graphical representation of the morphology of the combined computational model is shown in Figure 3.1. It features nine parameters, each representing an ion channel present in the model. In biological neurons, ion channels open and close in response to various changing physiological factors in and around the neuron. Figure 3.2, originally from [19] and used here under license:
CC BY 4.0 (https://creativecommons.org/licenses/by/4.0/), shows an example of ion channels on the membrane of a motoneuron. Ion channels play an important role in forming the action potential generated by the neuron. A change in one or more of the parameter values represents a new model. The parameters and base conductance values are shown in Table 3.1. These conductance values were established as part of the Kole model and further hand-tuned by Dr. Smolinski's students so that the desired action potential behavior was observed when an appropriate current was injected.

Each of the conductance values shown in Table 3.1 corresponds to an ion channel present in the model. This specific group of conductances together constitutes the base model parameters from which all the generated models' parameters were derived. The model's ion channels are designed to replicate biological ion channels. na_segment is a sodium channel on the axon initial segment. na_soma is a sodium channel on the soma. na_node is a sodium channel on the Nodes of Ranvier. Km_soma and Km_axon are based on muscarinic potassium channels on the soma

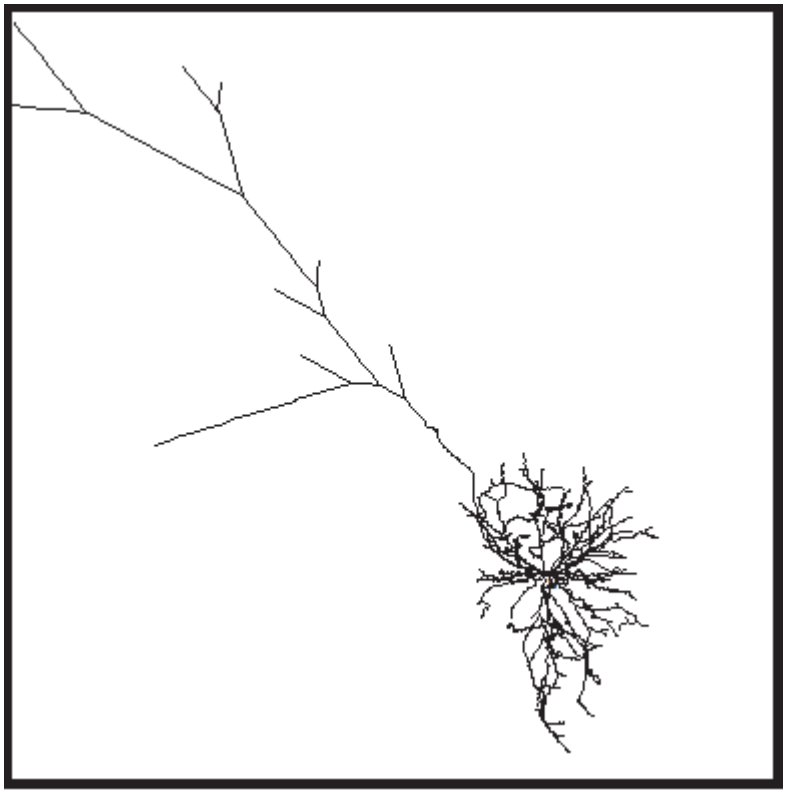

Figure 3.1: Graphical representation of the morphology of the motoneuron computational model that served as the basis for all generated models in this thesis.

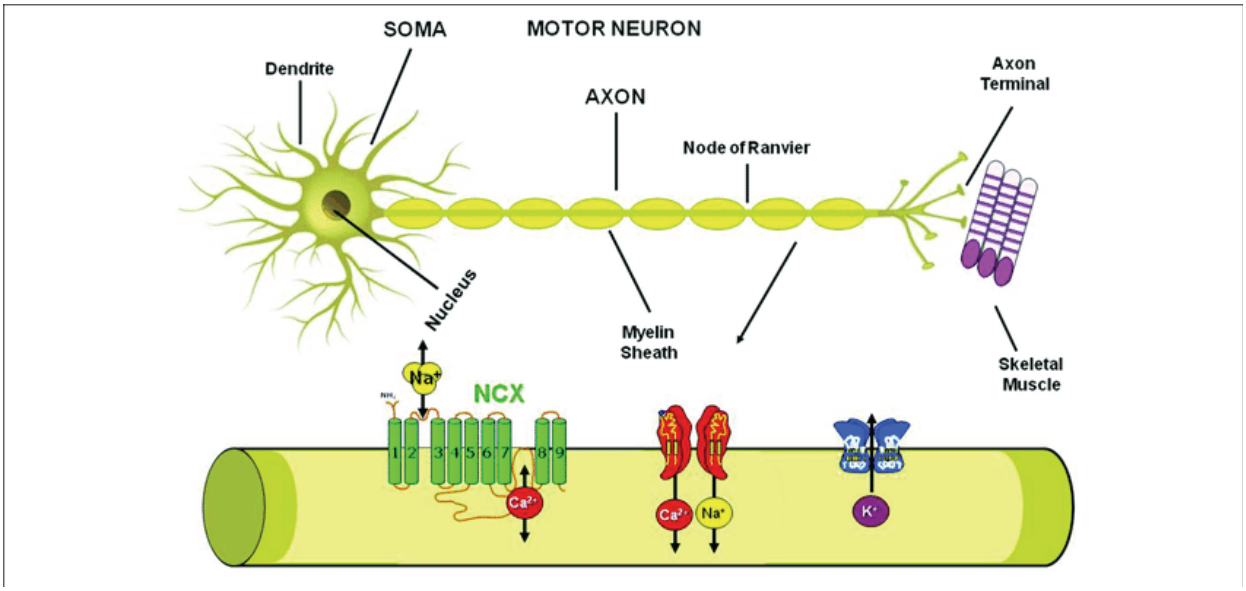

Figure 3.2: Plasmamembrane ion channels and transporters in the Motor Neuron. Scheme representing the axon structure and the distribution in the motor neuron plasmamembrane of Na^+/Ca^{2+} exchanger, Na^+, Ca^{2+} and K^+ channels. This figure is originally from [19] and used here under license:
CC BY 4.0 (https://creativecommons.org/licenses/by/4.0/).

Model Parameters		
Biological Ion Channel	**Model Parameter**	**Base Conductance Value**
Sodium channel on axon initial segment	na_segment	400 pS/µm^2
Sodium channel on soma	na_soma	60 pS/µm^2
Sodium channel on Nodes of Ranvier	na_node	2500 pS/µm^2
Muscarinic potassium channel on soma	Km_soma	5 pS/µm^2
Muscarinic potassium channel on axon	Km_axon	50 pS/µm^2
Voltage-gated potassium channel on soma	Kv_soma	20 pS/µm^2
Voltage-gated potassium channel on axon	Kv_axon	2000 pS/µm^2
Potassium channel from Kv1.1 subunits on soma	Kv1_soma	0.01 S/cm^2
Potassium channel from Kv1.1 subunits on axon	Kv1_axon	0.20 S/cm^2

Table 3.1: Model parameters and base conductance values. These conductance values were established as part of the Kole model [20] and further hand-tuned by Dr. Smolinski's students, who developed the hybrid model used in this thesis, so that the desired action potential behavior was observed when an appropriate current was injected.

and axon, respectively. Kv_soma and Kv_axon are voltage-gated potassium channels located on the soma and axon, respectively. Kv1_soma and Kv1_axon are implementations of potassium channels from Kv1.1 subunits located on the soma and axon, respectively.

The model was written to be compatible with the Neuron simulation environment [5]. The simulation environment introduces a given electric current to the model. It will then track changes in the electric potentials (voltage trace) of both the soma and the axon of the model. The simulator can determine whether the injected current induces an action potential and can calculate the input resistance of the model. Action potentials are how neurons pass signals. Various signals are passed to the neuron via the dendrites. Those signals and other physiological factors may cause a depolarization of the cell, leading to an action potential being generated at the axon initial segment. The signal is propagated along the axon and is refreshed at the Nodes of Ranvier. Backpropagation also occurs causing an action potential spike in the soma. Figure 3.3 shows an example, from Treated Batch 1, of the voltage trace information that the Neuron simulation environment can collect while simulating current being introduced to a computational model. Most models began a simulation with a resting potential of approximately -70 mV; the simulator judges an action potential being induced when the voltage spikes from both the soma and the axon cross into positive territory. The -70 mV initial resting potential was chosen specifically by the model designer in order to achieve a membrane potential of -75 mV at the soma. Input resistance was calculated in accordance with Ohm's Law.

$$Resistance = Voltage/Current$$

Threshold current (the smallest current which induces an action potential) was one of the objectives of the genetic algorithm. This was achieved by, for each computational model, running a simulation with incrementally higher current until an action potential spike was detected. The injection of the current was delayed by 300 ms on each simulation. The incremental current injection for the control batches began at 0.015 nA and stepped up by 0.015 nA to a maximum of 0.24 nA. The incremental current injection for the treated batches began at 0.14 nA and stepped up by 0.02

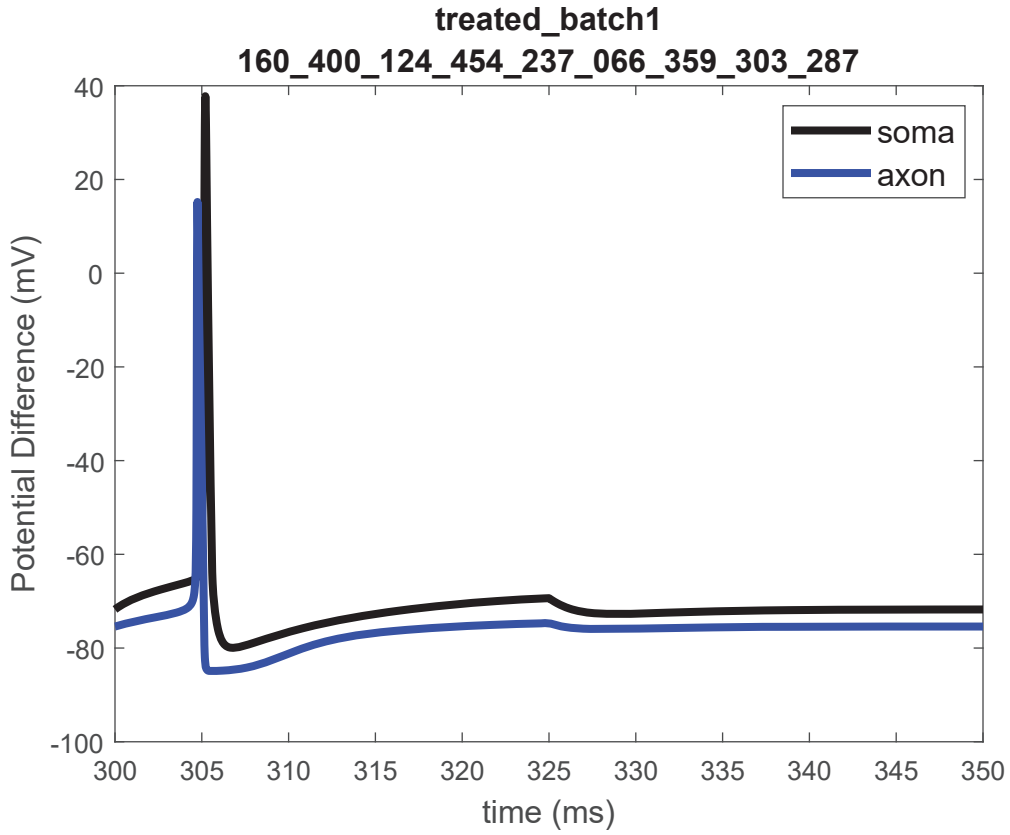

Figure 3.3: An example, from Treated Batch 1, of the voltage trace information Neuron can capture. This model had the following parameter gene values: na_segment = 160; na_soma = 400; na_node = 124; Km_soma = 454; Km_axon = 237; Kv_soma = 66; Kv_axon = 359; Kv1_soma = 303; Kv1_axon = 287.

Acceptable Objective Value Ranges					
Control			**Treated**		
Objective	Minimum	Maximum	Objective	Minimum	Maximum
Threshold Current	0.1 nA	0.15 nA	Threshold Current	0.25 nA	0.35 nA
Input Resistance	47 MΩ	57 MΩ	Input Resistance	22 MΩ	28 MΩ

Table 3.2: Objective value ranges for good models, adapted from Figure 2D in [1].

nA to a maximum of 0.44 nA. The relevant values for that model were then recorded. The other objective to be optimized was input resistance. Ranges for what constituted acceptable values were adapted from Figure 2D in [1] and can be seen here in Table 3.2.

SECTION 3.2: GENETIC ALGORITHM

Genetic algorithms were first described by John Holland [3]. They are called such because they have, at their core, Darwinian survival of the fittest and use the language of biological genetics. Each computational model, or individual, is represented by a chromosome. The collection of chromosomes in a given generation is a population. Each chromosome is comprised of genes; in this case, the number of genes was set to the number of model parameter values (nine). For the purpose of this thesis, each gene represented a multiplier for its respective parameter, holding an integer value between 0 and 500. Therefore, each computational model was represented by nine integer values. When the model was simulated with Neuron, each gene value was converted to a percentage by dividing it by 100. This percentage was then multiplied to the appropriate base parameter value, as shown in Table 3.1, to create the new parameter value to be simulated.

$$NewParameterValue = BaseParameterValue * (GeneValue/100)$$

In this work, each of the batches had populations of 30 chromosomes and the criterion for stopping was 50 generations completed. Each group, both untreated (control) and treated, had three separate and distinct batch runs.

For each batch, a population was randomly initialized at the beginning of the algorithm. There

are three main operations used in the standard genetic algorithm: selection, crossover, and mutation. Selection is the way the algorithm decides which chromosomes carry forward to the next generation based upon some fitness evaluation. How fitness is defined will be specific to the objective or objectives being optimized; typically, a more desirable outcome for an objective will yield a higher fitness. The specific method that was used in this thesis is described in the next section. Generally, each chromosome, has a probability to be selected proportional to its fitness in a process referred to as roulette wheel selection. Crossover is the exchange of genetic material between two chromosomes, the chance of which happening is governed by some given probability. Mutation occurs when a gene randomly changes its value based upon some given probability. Crossover and mutation help promote genetic diversity and a more expansive search of the parameter space, increasing diversity and reducing crowding in the search space. A generalized form of a standard genetic algorithm, adapted from [24], is shown in Algorithm 1.

Algorithm 1: Standard genetic algorithm

```
begin
    initialize population;
    evaluate population for fitness;
    perform selection on population;
    generation ← 1;
    while stopping criterion not met do
        perform crossover on population;
        perform mutation on population;
        evaluate population for fitness;
        perform selection on population;
        generation ← generation + 1;
    end
end
```

Since there were two objectives that needed to be optimized in this work, a multi-objective genetic algorithm was deemed appropriate. The specific genetic algorithm which was used to generate the computational models is called elitist, non-dominated vector-evaluated genetic algorithm (end-VEGA) [17], which is an extension of vector-evaluated genetic algorithm (VEGA), devel-

oped by J. David Schaffer [25]. Essentially, VEGA split the population into subpopulations and evaluated fitness as a vector instead of a scalar. Each subpopulation optimized on a different part of the vector, allowing for multiple objectives to be optimized at once, albeit by different subpopulations. The elitism aspect meant that chromosomes with high fitness in both objectives were stored in an archive, which became part of the selection process, giving high-fitness models a chance to pass through into the next generation without being affected by crossover or mutation. end-VEGA modified the roulette wheel selection such that each model in the population appeared twice on the wheel, once for each objective. Each appearance's relative area on the wheel was proportional to its respective fitness for the given objective.

SECTION 3.3: FITNESS EVALUATION WITH FUZZY LOGIC

After the models were generated by the genetic algorithm and simulated with Neuron, they were evaluated for fitness. Since the objectives had ranges of values which are acceptable, the use of fuzzy sets was appropriate. Fuzzy sets were formalized by Lotfi Zadeh [4], expanding on earlier work by Jan Łukasiewicz and Alfred Tarski. Fuzzy logic allows for an element to have degrees of membership in one or more sets, instead of a binary 'yes' or 'no.' These membership values take the range of real numbers between 0 and 1, with 0 meaning not a member of the set and 1 meaning the element is completely in that set.

For this work, fuzzy membership functions were established for each objective, threshold current and input resistance. Each objective had three fuzzy sets associated with it: TOO_LOW, NORMAL, and TOO_HIGH. Values corresponding to these sets are based upon the minimum and maximum values from Table 3.2. A membership value of greater than 0.749 in the NORMAL fuzzy set was deemed as having met the objective. The fuzzy sets were established so that each objective's minimum and maximum acceptable values evaluate to a membership of 0.75. Figure 3.4 shows an example of how fuzzy memberships are determined using fuzzy membership functions. Fuzzy membership functions were created for each objective, for both untreated (control) models

and treated models. Figures 3.5, 3.6, 3.7, and 3.8 show the fuzzy membership functions used to evaluate the fitness of the computational models.

SECTION 3.4: NERVOLVER

NeRvolver is software, implemented primarily in C++, developed by Dr. Tomasz Smolinski and his students, and modified for this thesis. NeRvolver tied all the components together. It coordinated the genetic algorithm to create the computational model parameters, launched Neuron to simulate the models, calculated fuzzy memberships to evaluate the models, and would have extracted any rules (as described in the next section). NeRvolver can also be configured for fuzzy control in subsequent batch runs if rules are successfully extracted. It can also be used to track the success rates and effectiveness of rules placed in the fuzzy controller.

SECTION 3.5: DATA ANALYSIS

Once the genetic algorithm and all simulations were complete for a batch, the models were separated into two groups: those that demonstrated the desired action potential behavior and met both objectives (membership > 0.749 in both objective NORMAL fuzzy sets) and those that did not. The data were further processed to trim models deemed to be unreliable, models with data from either extreme of the current injection ranges, for both control and treated models. Data from the lower extreme of the current injection are unreliable because, in the context of this thesis, there was no way to know whether the value was the true threshold current or if the threshold current would have occurred at a lower current. The upper extreme of the current injection was also unreliable because, if action potential spiking was not detected, then the upper extreme of the current injection was recorded as the current threshold associated with that model. The control models with a recorded threshold current of 0.015 nA and 0.24 nA were cut away from the data set. Likewise, the treated models with recorded threshold currents of 0.14 nA and 0.44 nA were trimmed. This, along with the rule extraction, was done in NeRvolver as well as checked and

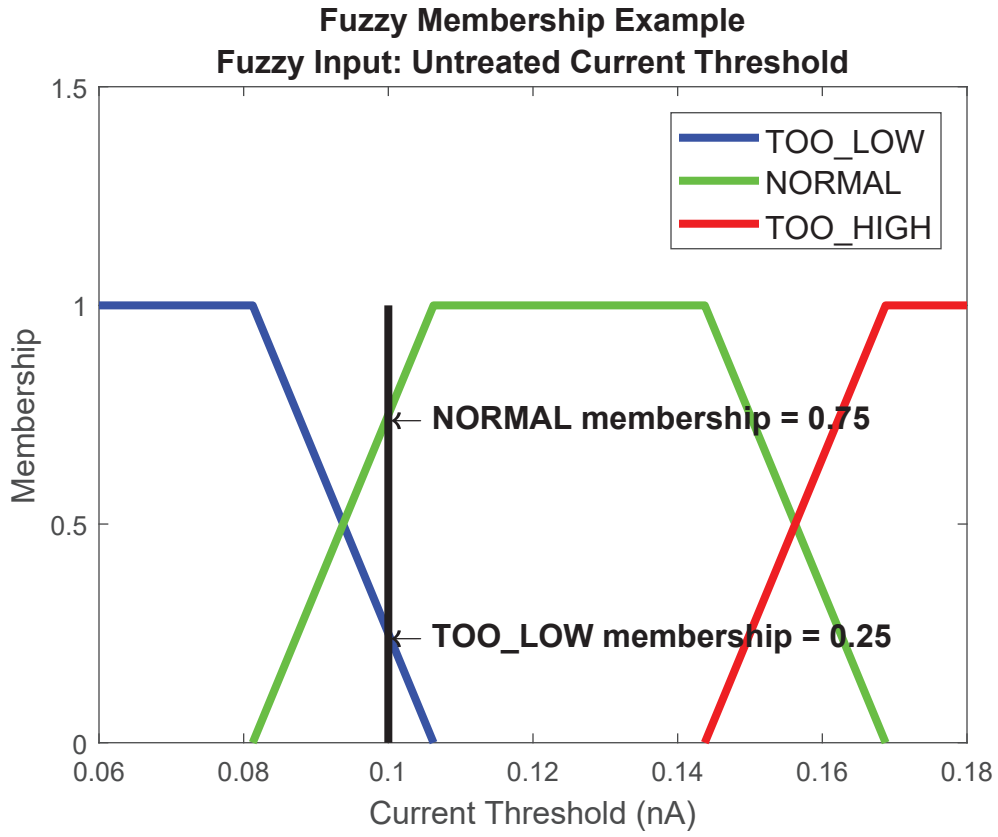

Figure 3.4: An example of how fuzzy memberships are determined using fuzzy membership functions. The three colored trapezoidal functions are the membership functions corresponding to each of the fuzzy sets for the untreated current threshold objective. In this example, the untreated motoneuron model resulted in a threshold current of 0.1 nA. This threshold current results in membership in two of the objective fuzzy sets: TOO_LOW and NORMAL. According to the fuzzy membership functions, TOO_LOW membership is calculated to be 0.25 and NORMAL membership is calculated to be 0.75. Since membership in the NORMAL fuzzy set is greater than 0.749, this model would meet the current threshold objective.

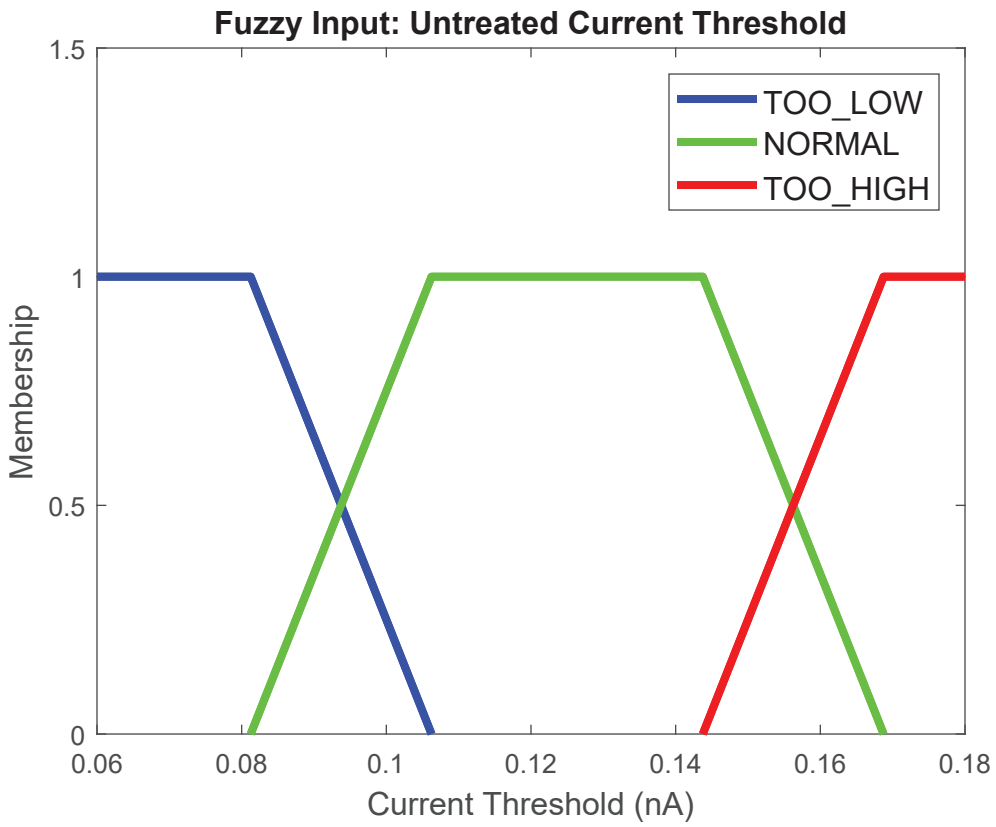

Figure 3.5: Fuzzy membership functions for the threshold current objective applicable to models in the Control group. A Control model with membership greater than 0.749 in the NORMAL fuzzy set was deemed as having met this objective.

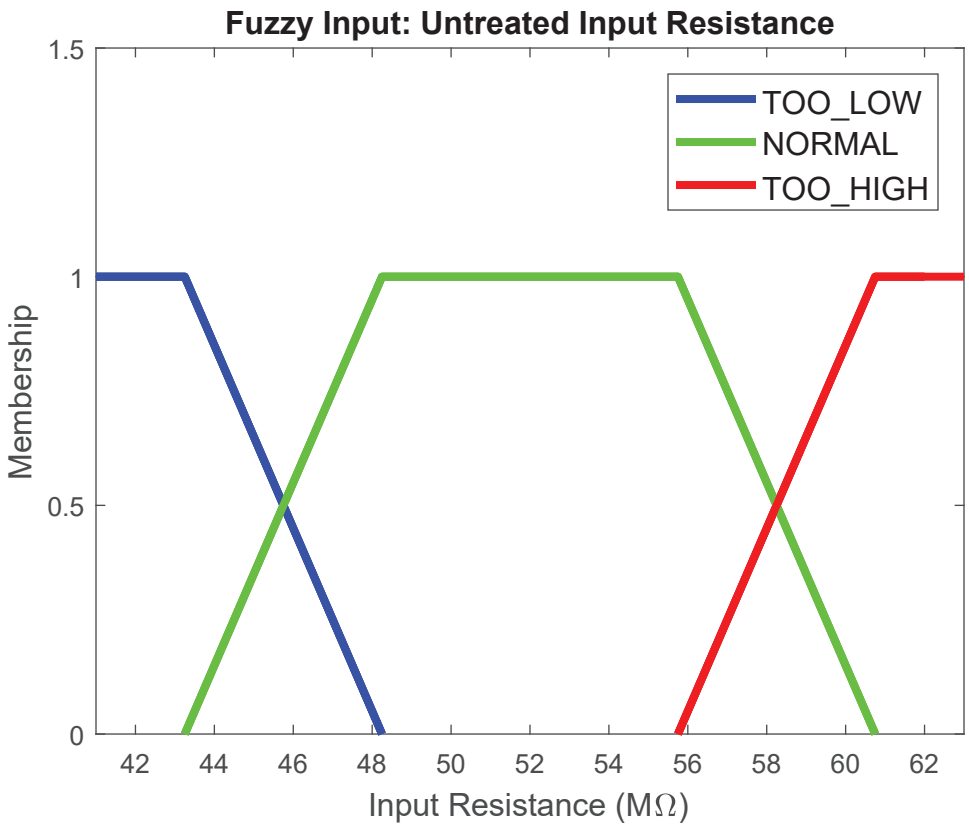

Figure 3.6: Fuzzy membership functions for the input resistance objective applicable to models in the Control group. A Control model with membership greater than 0.749 in the NORMAL fuzzy set was deemed as having met this objective.

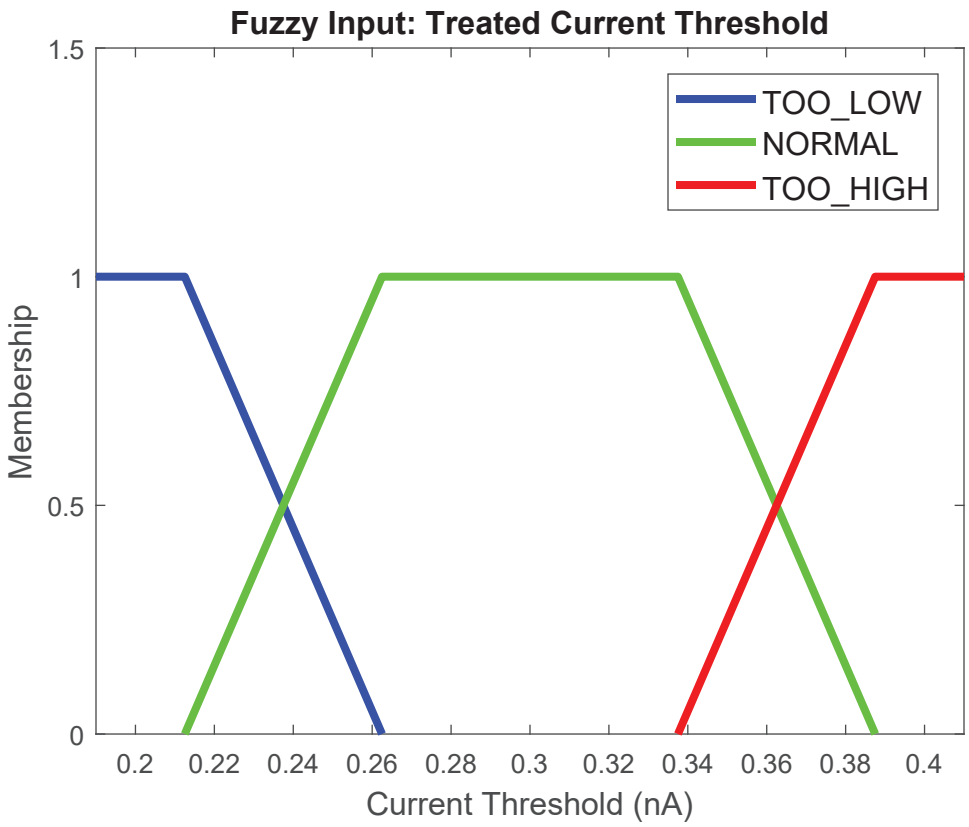

Figure 3.7: Fuzzy membership functions for the threshold current objective applicable to models in the Treated group. A Treated model with membership greater than 0.749 in the NORMAL fuzzy set was deemed as having met this objective.

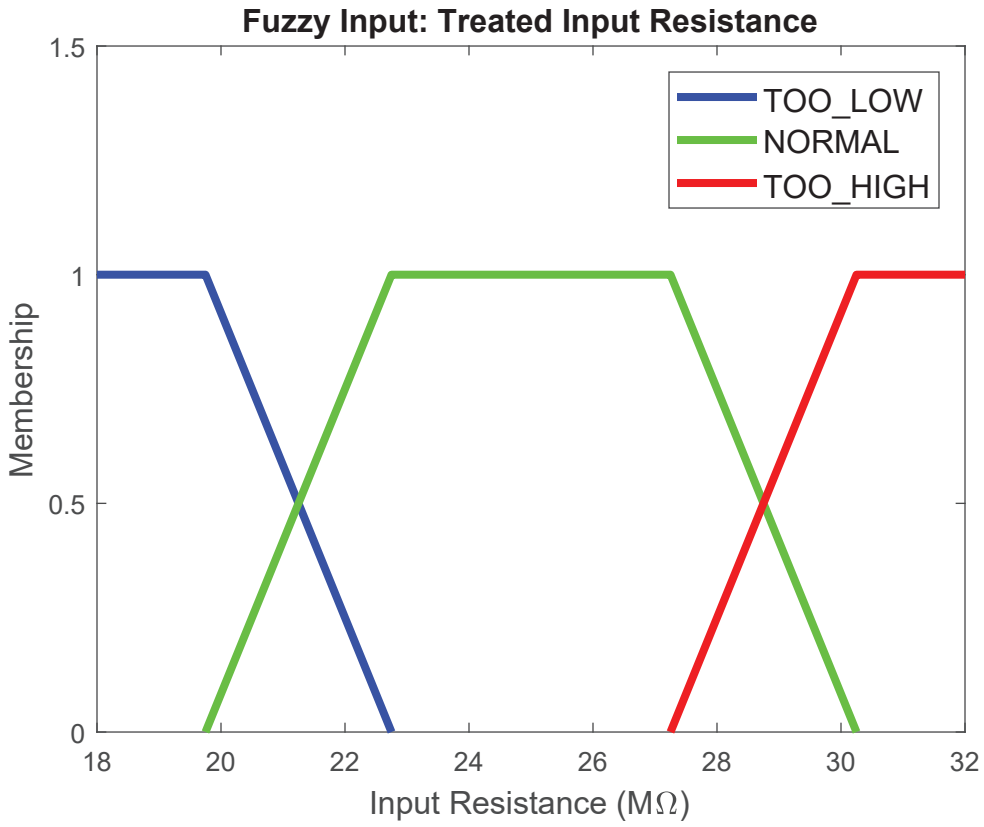

Figure 3.8: Fuzzy membership functions for the input resistance objective applicable to models in the Treated group. A Treated model with membership greater than 0.749 in the NORMAL fuzzy set was deemed as having met this objective.

verified with MATLAB.

To extract rules, the relationships between each of the objective fuzzy sets, specifically TOO_LOW and TOO_HIGH, and each of the parameter gene values of the corresponding models that had membership in that fuzzy set were examined. To accomplish this, a vector of memberships was created for each member of a given fuzzy set. The gene value for each corresponding parameter of members of that fuzzy set was added to its own vector. The Pearson correlation coefficient and p-value were calculated for each of the fuzzy membership and gene value combinations. If the absolute value of the correlation coefficient is greater than 0.7 and the p-value is less than 0.05, that suggests a rule to be extracted.

MATLAB was used to explore the relationships between each parameter and each other parameter, in each batch run, and as an entire control group and an entire treated group.

SECTION 3.6: PILOT TESTING

Preliminary testing was done with smaller batch runs for the purpose of identifying best practices when it came to the full-scale runs. Early batches ran for 10 generations with a population size of 20. Then, a setup with 20 generations with a population of 20 was tested. Finally, a setup with 30 generations with a population of 30 was tested before settling on the 50 generations and population of 30 that were used in the batches that are the subject of this thesis. Important things learned in the preliminary testing included being able to approximate the time a batch run would take, that many batches do not produce rules, and that many batches do not even produce models that meet the objectives.

Figure 3.9 shows an example of a correlation that produced a rule in preliminary testing. In this example, to reduce the model's membership in the Current_threshold_TOO_HIGH fuzzy set, one must increase the gene value of the na_segment parameter. So, the rule, put into words, becomes 'IF Current_threshold is TOO_HIGH, THEN INCREASE na_segment_par.'

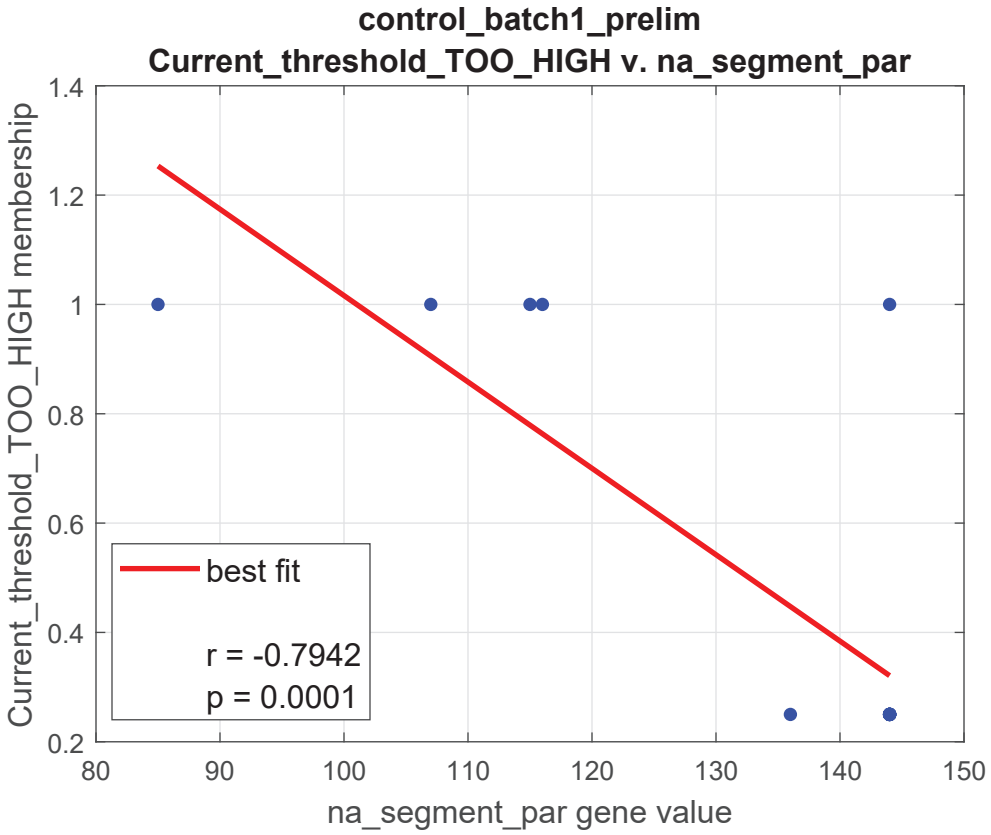

Figure 3.9: Example of a correlation which produced a rule in pilot testing. In this example, the gene for the sodium channel on the axon initial segment has a strong negative correlation with Current_threshold_TOO_HIGH fuzzy set membership. The inferred rule would be 'IF Current_threshold is TOO_HIGH, THEN INCREASE na_segment_par'.

SECTION 3.7: ASSUMPTIONS

In using the Pearson correlation, it is assumed that the relationship between the two variables is linear.

CHAPTER 4: RESEARCH FINDINGS

This chapter displays a per-batch breakdown of the number of models generated by each batch. The tables are broken down into good (models that exhibited the desired action potential spiking behavior and met both objectives) and bad (models that did not meet one or both objectives). The tables are also broken down into before and after trim. The data were trimmed following a batch run but before the data were analyzed. The trimmed data are unreliable, as described in the Data Analysis section of Chapter 3. The control models with a recorded threshold current of 0.015 nA and 0.24 nA were cut away from the data set. Likewise, the treated models with recorded threshold currents of 0.14 nA and 0.44 nA were trimmed.

Table 4.1 shows the number of models created for the individual Control (Untreated) batches and the combined Control group numbers.

Table 4.2 shows the number of models created for the individual Treated batches and the combined Treated group numbers.

No correlations between the parameter genes and the objective fuzzy sets were strong enough to yield any fuzzy rules. A complete enumeration of the correlation data can be found in the Appendix.

Figures in this chapter display relationships with strong correlations between the objectives and the parameters and within the parameters. Green markers represent models that exhibited appropriate action potential spiking and met both objectives. Red markers represent models that did not meet at least one objective.

Number of Control Models Generated		

Control (Untreated) Batch 1		
	Before Trim	**After Trim**
Good	126	126
Bad	837	258
Total	963	384

Control (Untreated) Batch 2		
	Before Trim	**After Trim**
Good	272	272
Bad	804	423
Total	1076	695

Control (Untreated) Batch 3		
	Before Trim	**After Trim**
Good	188	188
Bad	880	376
Total	1068	564

All Control (Untreated) Models		
	Before Trim	**After Trim**
Good	586	586
Bad	2521	1057
Total	3107	1643

Table 4.1: Numbers of Control models generated, broken down by batch and total Control group numbers.

Number of Treated Models Generated		

Treated Batch 1		
	Before Trim	**After Trim**
Good	436	436
Bad	689	159
Total	1125	595

Treated Batch 2		
	Before Trim	**After Trim**
Good	341	341
Bad	762	341
Total	1103	682

Treated Batch 3		
	Before Trim	**After Trim**
Good	366	366
Bad	613	109
Total	979	475

All Treated Models		
	Before Trim	**After Trim**
Good	1143	1143
Bad	2064	609
Total	3207	1752

Table 4.2: Numbers of Treated models generated, broken down by batch and total Treated group numbers.

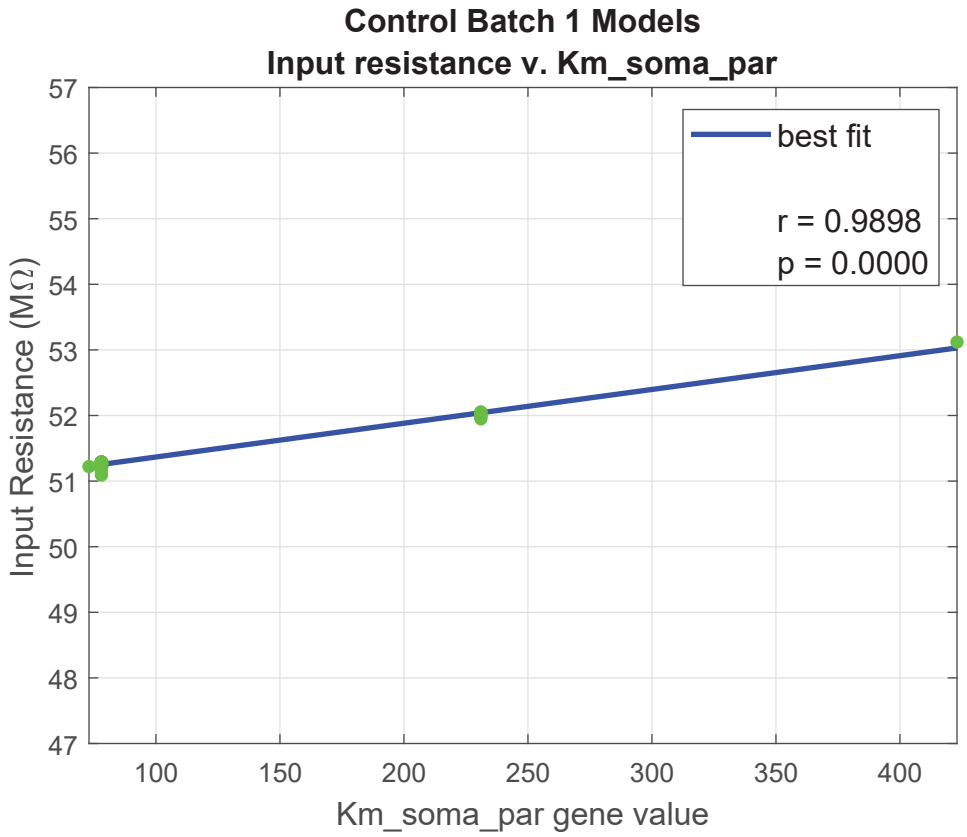

Figure 4.1: A strong correlation between the model parameter gene value of the muscarinic potassium channel on the soma and the value for input resistance in Control Batch 1. Green markers represent "good" models, which exhibited the desired spiking action potential behavior and met both objectives. Only "good" models were used to calculate this correlation. Each marker may be representative of multiple models. This relationship only appears in this batch.

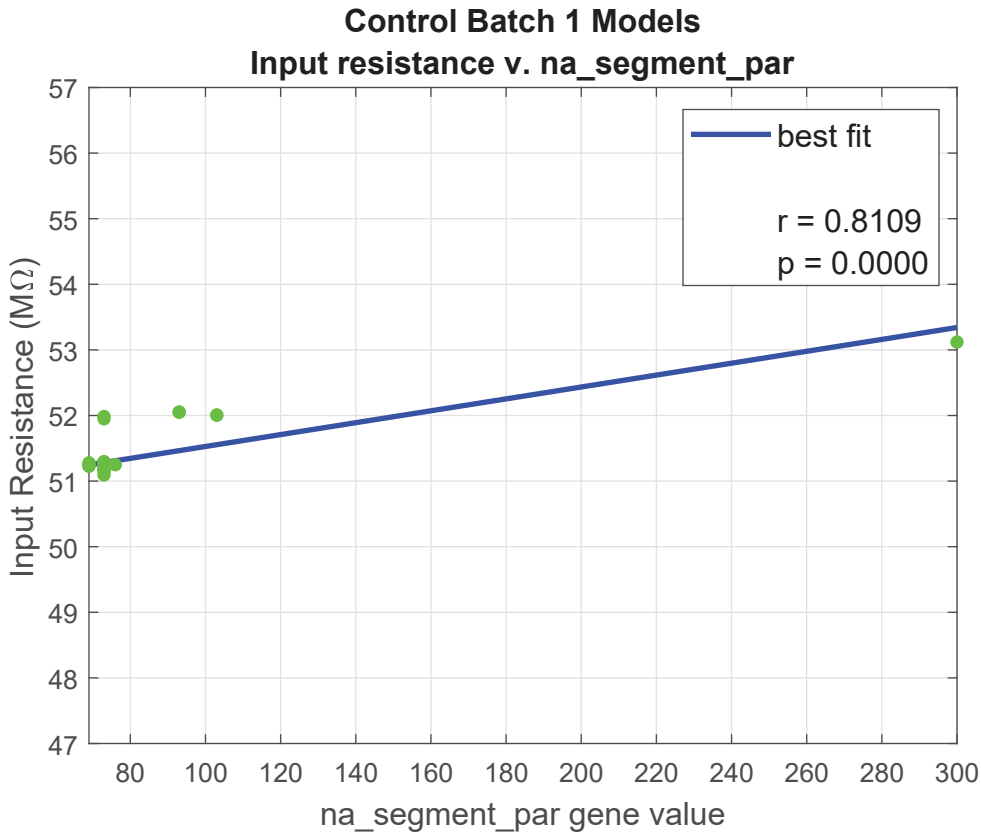

Figure 4.2: A strong correlation between the model parameter gene value of the sodium channel on the axon initial segment and the value for input resistance in Control Batch 1. Green markers represent "good" models, which exhibited the desired spiking action potential behavior and met both objectives. Only "good" models were used to calculate this correlation. Each marker may be representative of multiple models. This relationship only appears in this batch.

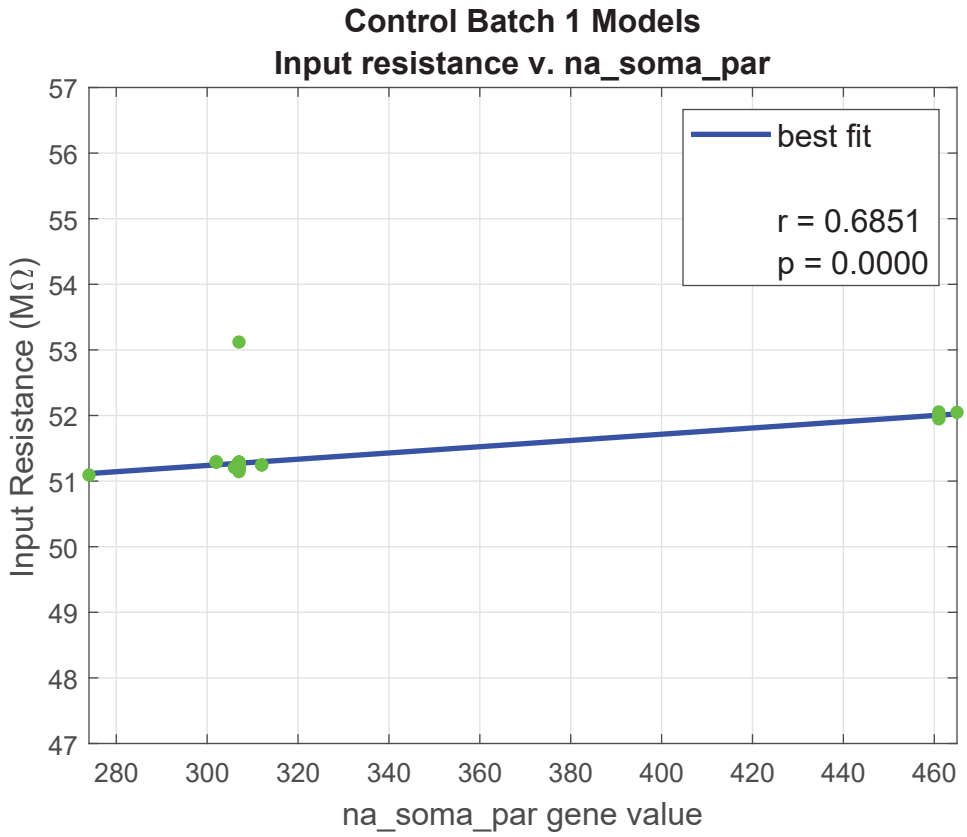

Figure 4.3: A strong correlation between the model parameter gene value of the sodium channel on the soma and the value for input resistance in Control Batch 1. Green markers represent "good" models, which exhibited the desired spiking action potential behavior and met both objectives. Only "good" models were used to calculate this correlation. Each marker may be representative of multiple models. This relationship only appears in this batch.

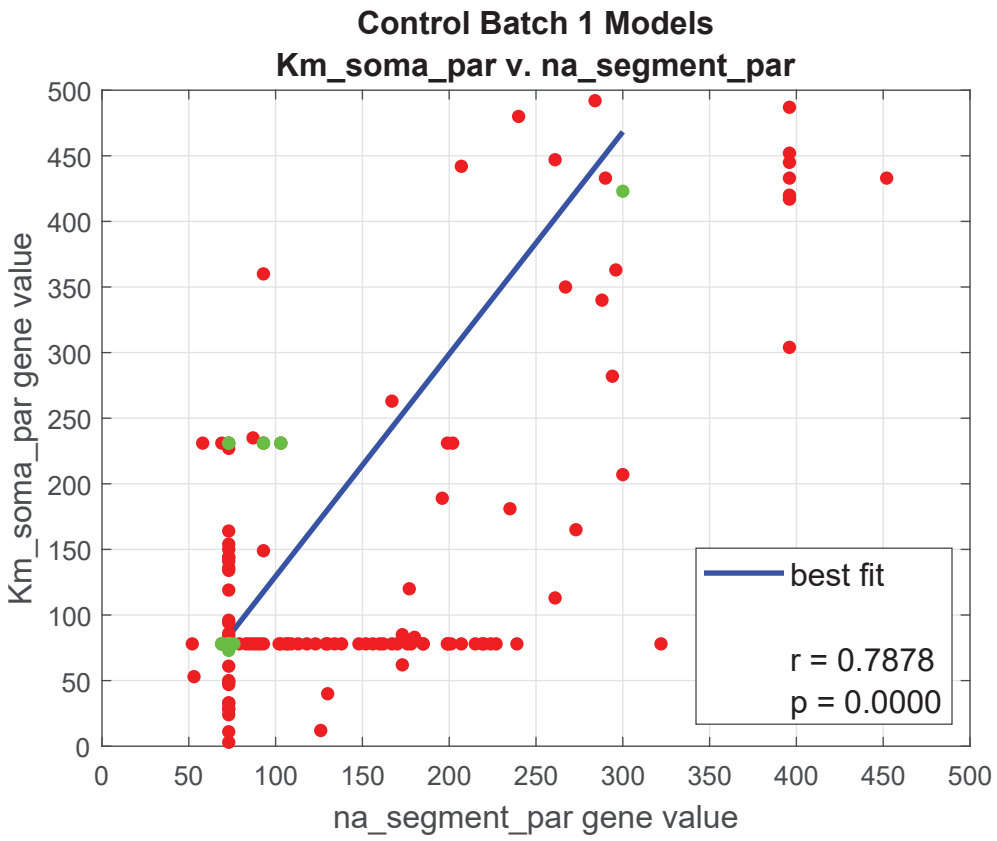

Figure 4.4: A strong correlation between the model parameter gene value of the sodium channel on the axon initial segment and the model parameter gene value of the muscarinic potassium channel on the soma in Control Batch 1. Green markers represent "good" models, which exhibited the desired spiking action potential behavior and met both objectives. Red markers represent "bad" models, which did not meet both objectives. Only "good" models were used to calculate this correlation. Each marker may be representative of multiple models. This relationship only appears in this batch.

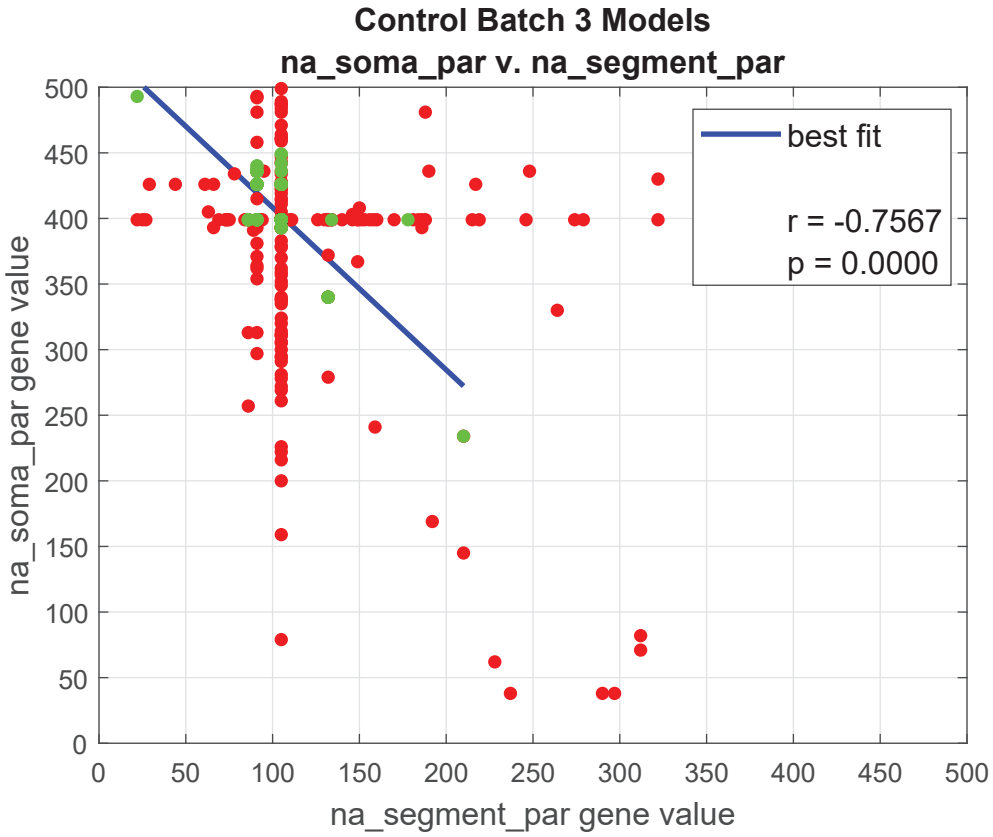

Figure 4.5: A strong correlation between the model parameter gene value of the sodium channel on the axon initial segment and the model parameter gene value of the sodium channel on the soma in Control Batch 3. Green markers represent "good" models, which exhibited the desired spiking action potential behavior and met both objectives. Red markers represent "bad" models, which did not meet both objectives. Only "good" models were used to calculate this correlation. Each marker may be representative of multiple models. This relationship only appears in this batch.

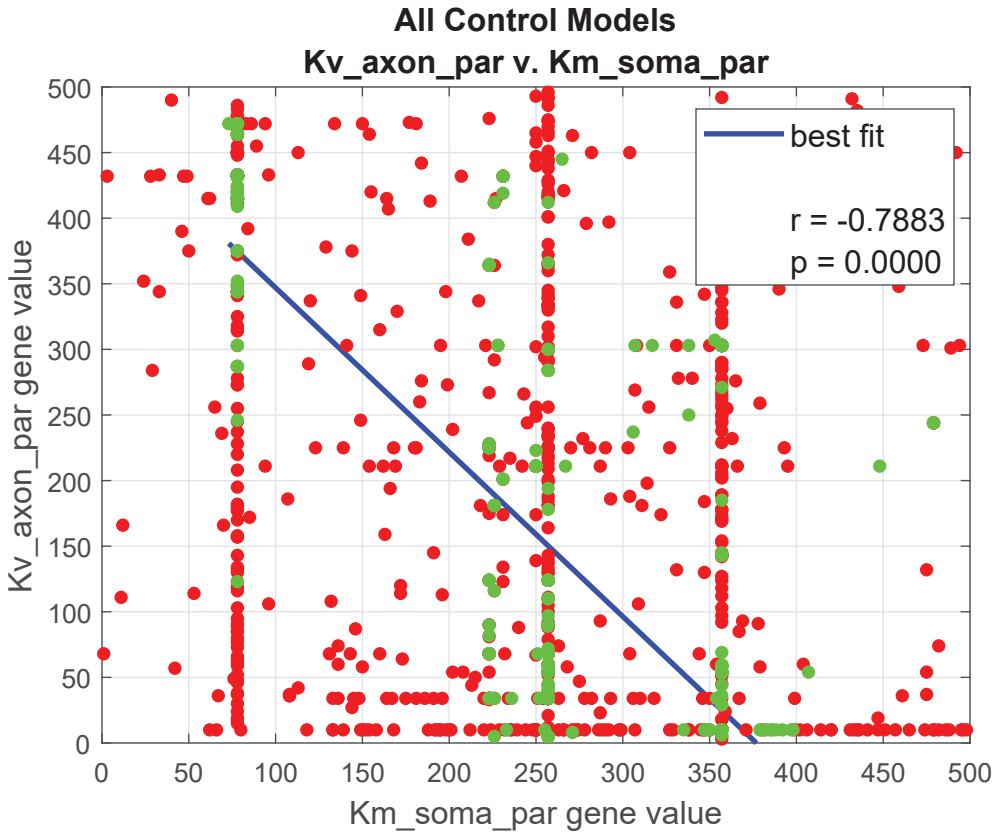

Figure 4.6: A strong correlation between the model parameter gene value of the muscarinic potassium channel on the soma and the model parameter gene value of the voltage-gated potassium channel on the axon in the combined Control group. Green markers represent "good" models, which exhibited the desired spiking action potential behavior and met both objectives. Red markers represent "bad" models, which did not meet both objectives. Only "good" models were used to calculate this correlation. Each marker may be representative of multiple models. This relationship only appears in this experimental group.

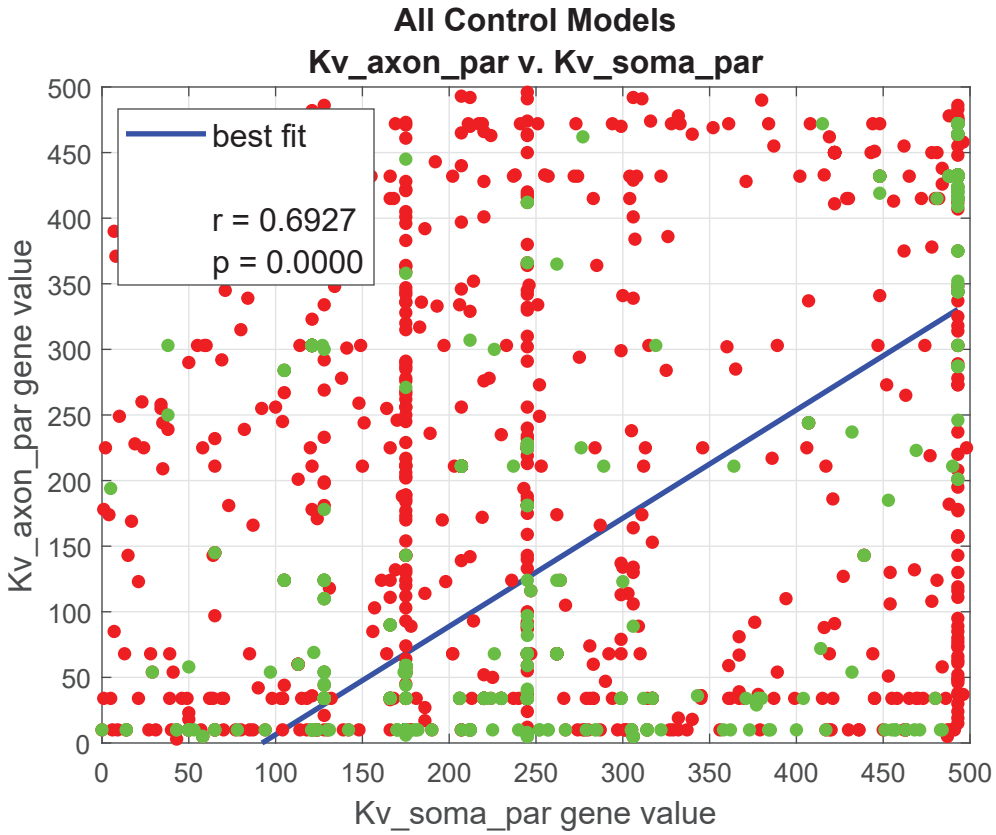

Figure 4.7: A strong correlation between the model parameter gene value of the voltage-gated potassium channel on the soma and the model parameter gene value of the voltage-gated potassium channel on the axon in the combined Control group. Green markers represent "good" models, which exhibited the desired spiking action potential behavior and met both objectives. Red markers represent "bad" models, which did not meet both objectives. Only "good" models were used to calculate this correlation. Each marker may be representative of multiple models. This relationship only appears in this experimental group.

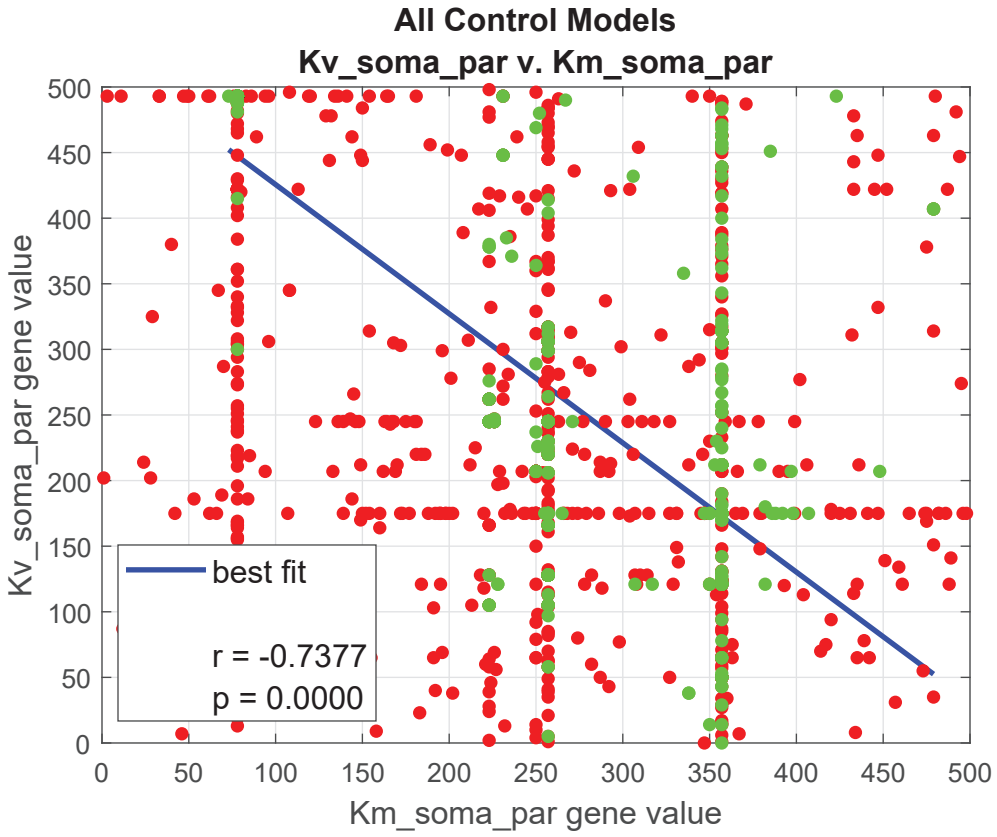

Figure 4.8: A strong correlation between the model parameter gene value of the muscarinic potassium channel on the soma and the model parameter gene value of the voltage-gated potassium channel on the soma in the combined Control group. Green markers represent "good" models, which exhibited the desired spiking action potential behavior and met both objectives. Red markers represent "bad" models, which did not meet both objectives. Only "good" models were used to calculate this correlation. Each marker may be representative of multiple models. This relationship only appears in this experimental group.

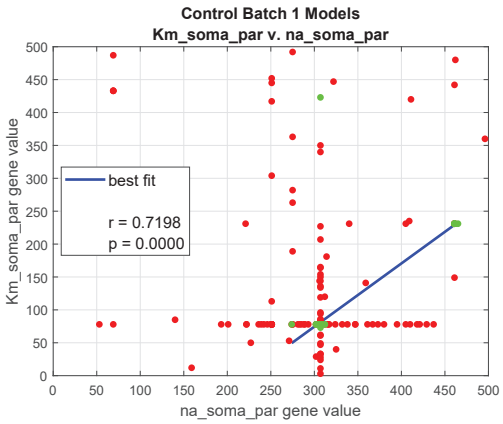

Figure 4.9: A strong correlation between the model parameter gene value of the sodium channel on the soma and the model parameter gene value of the muscarinic potassium channel on the soma in Control Batch 1. Green markers represent "good" models, which exhibited the desired spiking action potential behavior and met both objectives. Red markers represent "bad" models, which did not meet both objectives. Only "good" models were used to calculate this correlation. Each marker may be representative of multiple models. This relationship also appears in Treated Batch 1 in a different area of the parameter space.

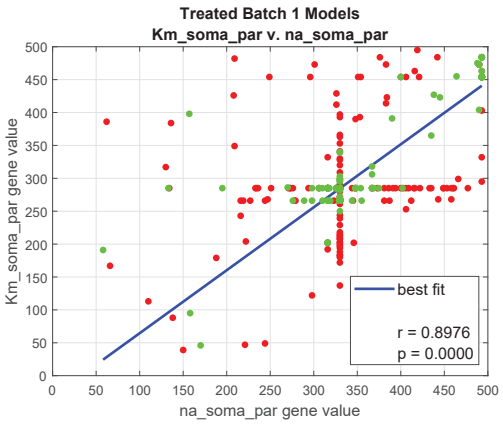

Figure 4.10: A strong correlation between the model parameter gene value of the sodium channel on the soma and the model parameter gene value of the muscarinic potassium channel on the soma in Treated Batch 1. Green markers represent "good" models, which exhibited the desired spiking action potential behavior and met both objectives. Red markers represent "bad" models, which did not meet both objectives. Only "good" models were used to calculate this correlation. Each marker may be representative of multiple models. This relationship also appears in Control Batch 1 in a different area of the parameter space.

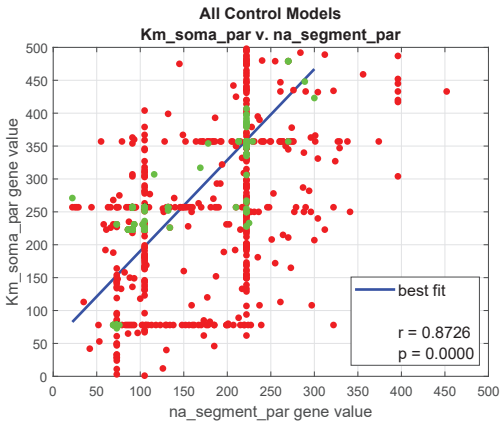

Figure 4.11: A strong correlation between the model parameter gene value of the sodium channel on the axon initial segment and the model parameter gene value of the muscarinic potassium channel on the soma in the combined Control group. Green markers represent "good" models, which exhibited the desired spiking action potential behavior and met both objectives. Red markers represent "bad" models, which did not meet both objectives. Only "good" models were used to calculate this correlation. Each marker may be representative of multiple models. This relationship also appears in the combined Treated group in a different area of the parameter space. With this strong relationship appearing in both respective combined experimental groups, it may suggest a possible co-regulation of the biological genes that express these ion channels.

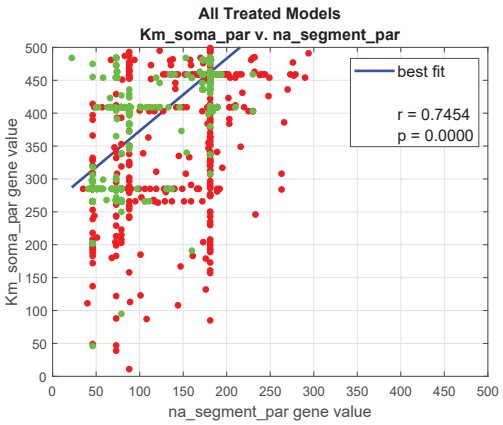

Figure 4.12: A strong correlation between the model parameter gene value of the sodium channel on the axon initial segment and the model parameter gene value of the muscarinic potassium channel on the soma in the combined Treated group. Green markers represent "good" models, which exhibited the desired spiking action potential behavior and met both objectives. Red markers represent "bad" models, which did not meet both objectives. Only "good" models were used to calculate this correlation. Each marker may be representative of multiple models. This relationship also appears in the combined Control group in a different area of the parameter space. With this strong relationship appearing in both respective combined experimental groups, it may suggest a possible co-regulation of the biological genes that express these ion channels.

CHAPTER 5: CONCLUSIONS

SECTION 5.1: SUMMARY

This thesis work addressed the challenge of exploring the intrinsic changes that spinal motoneurons undergo following a period of persistent activation, a process which can be mimicked in a laboratory setting by treating the motoneurons with high K^+. Understanding how motoneurons change under these conditions has implications in fields such as medicine, robotics, and other fields using biologically-inspired models.

A multi-objective genetic algorithm was used to manipulate a computational model's ion channels to generate new computational models. Nine ion channels were identified as the parameters for the models. The objectives to be optimized were identified as the threshold current (to induce an action potential) and input resistance. Two experimental groups were established: one of computational models representing dormant (control) motoneurons and one of computational models representing motoneurons treated with high K^+ (mimicking persistent activation). Fuzzy logic was used to assign memberships in each objective fuzzy set to each generated model and evaluate each model's fitness over the two objectives.

Correlations were drawn between the TOO_LOW and TOO_HIGH fuzzy sets of each objective and each parameter to mine fuzzy rules which could be used to compare the two experimental groups. Importantly, examination was given to relationships between the objectives and parameters within and across the two experimental groups.

SECTION 5.2: CONCLUSIONS AND DISCUSSION

Exploring the correlations between the objective fuzzy sets and the model parameters did not yield any correlations strong enough to imply any fuzzy rules. Small-scale testing was able show that the method used in this thesis can mine fuzzy rules. One likely explanation for the lack of results with the fuzzy rules is small sample size. The parameter space is large, nine-dimensional,

and evaluated over two objectives. The problem becomes a tradeoff of time and computational resources for an increase in model generation. Simulating and evaluating the models is expensive, in terms of time and computational resources. Getting larger populations of computational models would be beneficial.

It is not just a problem of the number of models, but also of the diversity of the models. Once the genetic algorithm identifies a highly-fit model, it replicates that model with minor variations, creating distinct models that are not very diverse. Crossover and mutation can only go so far to combat this. One solution could be to monitor for crowding in the search space and introduce methods to force models away from crowded areas. Another solution could be to introduce harsher fitness penalties for models in a crowded area of the search space. A less ideal method would be to identify clustered models after the batch run has complete and evaluate those models again with varied parameter values.

Interesting results in this research were found when an examination was made of the relationships between the objective values and parameter gene values of the good models. Figures 4.1, 4.2, 4.3, 4.4, and 4.5 show relationships that only exist in a control batch, but not in the other control batches or in the treated batches. The suggestion here is that it is possible that some relationships may only exist within a specific area of the parameter space, but not in other areas.

Figures 4.6, 4.7, and 4.8 show relationships that exist when the three Control batches were combined, but do not appear when looking at the Treated models. These relationships may provide clues as to the types of changes that ion channels undergo following persistent activation.

There are two relationships that appear when examining both the Control and Treated models. The Km_soma channel and the na_soma channel are both positively correlated in Control Batch 1 and Treated Batch 1, as shown in Figures 4.9 and 4.10. Perhaps more interesting is the relationship between the Km_soma channel and the na_segment channel. This relationship is seen in both the combined Control group and the combined Treated group, as shown in Figures 4.11 and 4.12. These relationships, existing in both experimental groups, may suggest a deep link between these

ion channels such as a possible co-regulation of the genes that express these ion channels.

SECTION 5.3: SUGGESTIONS FOR FUTURE RESEARCH

Future work should look to using an updated computational model. The model published along with [18] seems like a likely candidate. The publication and the model are recent and may be easier to implement in a similar manner as this thesis work.

A third objective may need to be considered, namely, the resting potential of the motoneuron model. This thesis paid little attention to the resting potential, as it was more concerned with threshold current and input resistance. Including resting potential as an objective may bring this method closer to results seen in wet labs with actual motoneuron samples.

Including methods to increase diversity of generated models, like those discussed in the previous section, would greatly improve the results of examining objective and parameter relationships and correlations.

It may be interesting to create and include experimental groups representing motoneurons with acceptable objective values in between the control group and treated group of this thesis. The purpose would be to investigate the "micro-rules" of these in-between states, when and where these rules appear and disappear.

One of the original intentions of this thesis work was to include a fuzzy controller to improve model quality during the evolutionary process. Time and implementation issues prevented that from happening. Implementing a fuzzy output set like the example shown in Figure 5.1 to improve gene values during evolution would help with gaining quicker convergence on good models. Known rules would be given to the fuzzy controller and models that trigger rules may benefit from the modifier the fuzzy controller applies to the triggered parameter gene. Software libraries such as FuzzyLite [26] could be utilized for this purpose.

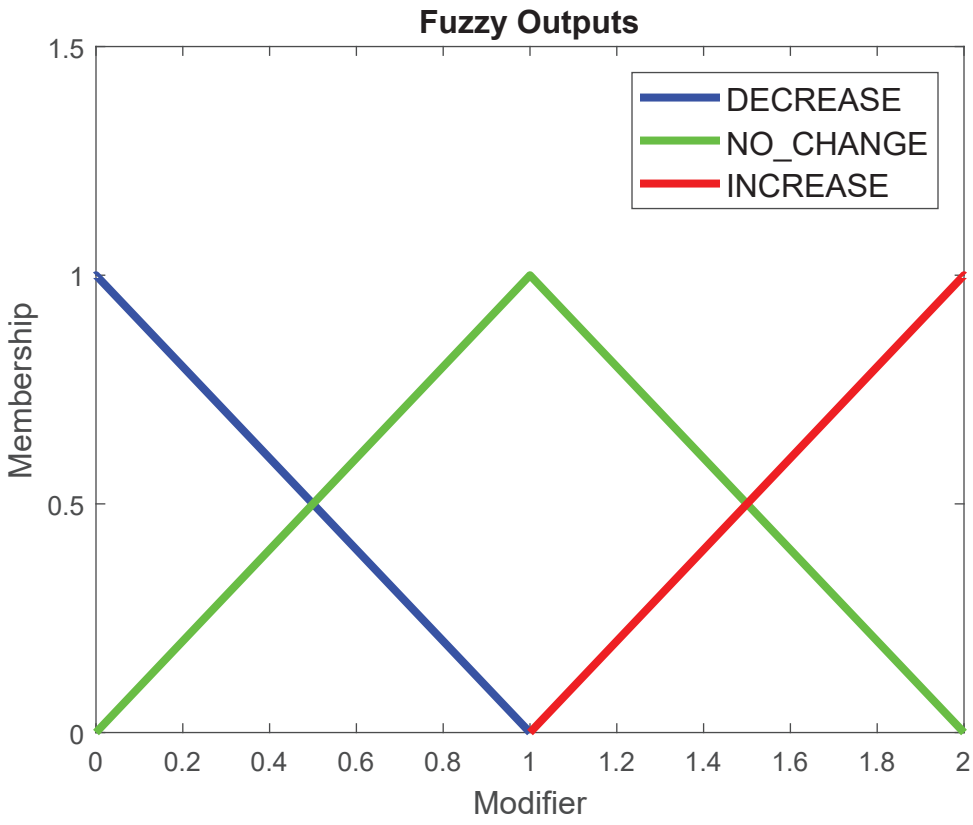

Figure 5.1: Potential membership functions for fuzzy output sets for use with a fuzzy controller.

REFERENCES

[1] M. A. Harrington and T. G. Smolinski, "Mechanisms and modeling of the adaptive modulation of the intrinsic properties of spinal motoneurons," Research grant proposal for Collaborative Research in Computational Neuroscience, National Science Foundation, 2016.

[2] P. Patel, "Hybridization of multi-objective evolutionary algorithms and fuzzy control for automated construction, tuning, and analysis of neuronal models," Master's thesis, Delaware State University, 2013.

[3] J. H. Holland, *Adaptation in Natural and Artificial Systems*. The University of Michigan, 1975.

[4] L. A. Zadeh, "Fuzzy sets," *Information and Control*, vol. 8, no. 3, pp. 338–353, Jun. 1965, ISSN: 0019-9958. DOI: 10.1016/S0019-9958(65)90241-X. [Online]. Available: https://www.sciencedirect.com/science/article/pii/S001999586590241X.

[5] N. T. Carnevale and M. L. Hines, *The Neuron Book*. Cambridge University Press, 2009, ISBN: 978-0-521-11563-6.

[6] A. L. Hodgkin, A. F. Huxley, and B. Katz, "Measurement of current-voltage relations in the membrane of the giant axon of loligo," *The Journal of Physiology*, vol. 116, no. 4, pp. 424–448, 1952. DOI: 10.1113/jphysiol.1952.sp004716. eprint: https://physoc.onlinelibrary.wiley.com/doi/pdf/10.1113/jphysiol.1952.sp004716. [Online]. Available: https://physoc.onlinelibrary.wiley.com/doi/abs/10.1113/jphysiol.1952.sp004716.

[7] A. L. Hodgkin and A. F. Huxley, "Currents carried by sodium and potassium ions through the membrane of the giant axon of loligo," *The Journal of Physiology*, vol. 116, no. 4, pp. 449–472, 1952. DOI: 10.1113/jphysiol.1952.sp004717. eprint: https://physoc.onlinelibrary.wiley.com/doi/pdf/10.1113/jphysiol.1952.sp004717. [Online]. Available: https://physoc.onlinelibrary.wiley.com/doi/abs/10.1113/jphysiol.1952.sp004717.

[8] A. L. Hodgkin and A. F. Huxley, "The components of membrane conductance in the giant axon of loligo," *The Journal of Physiology*, vol. 116, no. 4, pp. 473–496, 1952. DOI: 10.1113/jphysiol.1952.sp004718. eprint: https://physoc.onlinelibrary.wiley.com/doi/pdf/10.1113/jphysiol.1952.sp004718. [Online]. Available: https://physoc.onlinelibrary.wiley.com/doi/abs/10.1113/jphysiol.1952.sp004718.

[9] A. L. Hodgkin and A. F. Huxley, "The dual effect of membrane potential on sodium conductance in the giant axon of loligo," *The Journal of Physiology*, vol. 116, no. 4, pp. 497–506, 1952. DOI: 10.1113/jphysiol.1952.sp004719. eprint: https://physoc.onlinelibrary.wiley.com/doi/pdf/10.1113/jphysiol.1952.sp004719. [Online]. Available: https://physoc.onlinelibrary.wiley.com/doi/abs/10.1113/jphysiol.1952.sp004719.

[10] A. L. Hodgkin and A. F. Huxley, "A quantitative description of membrane current and its application to conduction and excitation in nerve," *The Journal of Physiology*, vol. 117, no. 4, pp. 500–544, 1952. DOI: 10.1113/jphysiol.1952.sp004764. eprint: https://physoc.onlinelibrary.wiley.com/doi/pdf/10.1113/jphysiol.1952.sp004764. [Online]. Available: https://physoc.onlinelibrary.wiley.com/doi/abs/10.1113/jphysiol.1952.sp004764.

[11] J. S. Carp, X.-Y. Chen, H. Sheikh, and J. R. Wolpaw, "Operant conditioning of rat h-reflex affects motoneuron axonal conduction velocity," *Experimental Brain Research*, vol. 136, pp. 269–273, 2001. DOI: 10.1007/s002210000608.

[12] J. S. Carp and J. R. Wolpaw, "Motoneuron plasticity underlying operantly conditioned decrease in primate h-reflex," *Journal of Neurophysiology*, vol. 72, no. 1, pp. 431–442, 1994. DOI: 10.1152/jn.1994.72.1.431. [Online]. Available: https://www.physiology.org/doi/abs/10.1152/jn.1994.72.1.431.

[13] E. Beaumont and P. F. Gardiner, "Endurance training alters the biophysical properties of hindlimb motoneurons in rats," *Muscle & Nerve*, vol. 27, no. 2, pp. 228–236, 2003. DOI: 10.1002/mus.10308. eprint: https://onlinelibrary.wiley.com/doi/pdf/10.1002/mus.10308. [Online]. Available: https://onlinelibrary.wiley.com/doi/abs/10.1002/mus.10308.

[14] P. Gardiner, E. Beaumont, and B. Cormery, "Motoneurones "learn" and "forget" physical activity," *Canadian Journal of Applied Physiology*, vol. 30, no. 3, pp. 352–370, 2005. DOI: 10.1139/h05-127.

[15] C. W. MacDonell, D. C. Button, E. Beaumont, B. Cormery, and P. F. Gardiner, "Plasticity of rat motoneuron rhythmic firing properties with varying levels of afferent and descending inputs," *Journal of Neurophysiology*, vol. 107, no. 1, pp. 265–272, Jan. 2012. DOI: 10.1152/jn.00122.2011. eprint: https://www.physiology.org/doi/pdf/10.1152/jn.00122.2011. [Online]. Available: https://www.physiology.org/doi/full/10.1152/jn.00122.2011.

[16] G. Le Masson, S. Przedborski, and L. F. Abbott, "A computational model of motor neuron degeneration," *Neuron*, vol. 83, no. 4, pp. 975–988, Aug. 2014. DOI: 10.1016/j.neuron.2014.07.001. [Online]. Available: https://www.cell.com/neuron/fulltext/S0896-6273(14)00582-0.

[17] T. G. Smolinski, G. M. Boratyn, M. Milanova, R. Buchanan, and A. A. Prinz, "Hybridization of independent component analysis, rough sets, and multi-objective evolutionary algorithms for classificatory decomposition of cortical evoked potentials," in *Pattern Recognition in Bioinformatics*, J. C. Rajapakse, L. Wong, and R. Acharya, Eds., Springer Berlin Heidelberg, 2006, pp. 174–183, ISBN: 978-3-540-37447-3.

[18] J. Lombardo, J. Sun, and M. A. Harrington, "Rapid activity-dependent modulation of the intrinsic excitability through up-regulation of kcnq/kv7 channel function in neonatal spinal motoneurons," *PLOS ONE*, vol. 13, no. 3, pp. 1–18, Mar. 2018. DOI: 10.1371/journal.pone.0193948. [Online]. Available: https://doi.org/10.1371/journal.pone.0193948.

[19] R. Sirabella, V. Valsecchi, S. Anzilotti, O. Cuomo, A. Vinciguerra, P. Cepparulo, P. Brancaccio, N. Guida, N. Blondeau, L. M. T. Canzoniero, C. Franco, S. Amoroso, L. Annunziato, and G. Pignataro, "Ionic homeostasis maintenance in als: Focus on new therapeutic targets," *Frontiers in Neuroscience*, vol. 12, Aug. 2018. DOI: 10.3389/fnins.2018.00510.

[20] M. H. P. Kole, S. U. Ilschner, B. M. Kampa, S. R. Williams, P. C. Ruben, and G. J. Stuart, "Action potential generation requires a high sodium channel density in the axon initial segment," *Nature Neuroscience*, vol. 11, pp. 178–186, Jan. 2008. DOI: 10.1038/nn2040. [Online]. Available: https://www.nature.com/articles/nn2040.

[21] Y. Li, D. Brewer, R. E. Burke, and G. A. Ascoli, "Developmental changes in spinal motoneuron dendrites in neonatal mice," *Journal of Comparative Neurology*, vol. 483, no. 3, pp. 304–317, 2005. DOI: 10.1002/cne.20438. eprint: https://onlinelibrary.wiley.com/doi/pdf/10.1002/cne.20438. [Online]. Available: https://onlinelibrary.wiley.com/doi/abs/10.1002/cne.20438.

[22] Computational Neuroanatomy Group, Center for Neural Informatics, Structures, and Placticity, Krasnow Institute for Advanced Study, George Mason University. (Nov. 2018). NeuroMorpho.Org. version 7.6, [Online]. Available: NeuroMorpho.Org.

[23] G. A. Ascoli, D. E. Donohue, and M. Halavi, "Neuromorpho.org: A central resource for neuronal morphologies," *Journal of Neuroscience*, vol. 27, no. 35, pp. 9247–9251, 2007, ISSN: 0270-6474. DOI: 10.1523/JNEUROSCI.2055-07.2007. eprint: http://www.jneurosci.org/content/27/35/9247.full.pdf. [Online]. Available: http://www.jneurosci.org/content/27/35/9247.

[24] L. N. de Castro, *Fundamentals of Natural Computing, Basic Concepts, Algorithms, and Applications*, S. Sahni, Ed., ser. Computer and Information Science. Chapman & Hall/CRC, 2006, ISBN: 1-58488-643-9.

[25] J. D. Schaffer, "Multiple objective optimization with vector evaluated genetic algorithms," in *Proceedings of the First Int. Conference on Genetic Algortihms*, Jan. 1985, pp. 93–100.

[26] J. Rada-Vilela, *Fuzzylite: A fuzzy logic control library*, 2017. [Online]. Available: http://fuzzylite.com/.

APPENDIX

The tables in this appendix show the per-batch breakdown of the correlations of each objective's (current threshold and input resistance) TOO HIGH and TOO LOW fuzzy sets and each of the parameters. Also shown are tables representing the combined batches of each group: Control (untreated) and Treated (with high K^+). Each row of the table shows the parameter, the objective fuzzy set, the number of models with membership in that objective fuzzy set, the Pearson correlation coefficient, and the p-value.

Control Batch 1 Fuzzy Correlations				
parameter	objective fuzzy set	number of models	correlation coef	p value
na segment par	Current threshold TOO LOW	129	0.2790	0.0014
na soma par	Current threshold TOO LOW	129	-0.0283	0.7504
na node par	Current threshold TOO LOW	129	0.0888	0.3170
Km soma par	Current threshold TOO LOW	129	0.0955	0.2818
Km axon par	Current threshold TOO LOW	129	-0.1843	0.0365
Kv soma par	Current threshold TOO LOW	129	-0.0125	0.8880
Kv axon par	Current threshold TOO LOW	129	0.0600	0.4993
Kv1 soma par	Current threshold TOO LOW	129	0.0891	0.3153
Kv1 axon par	Current threshold TOO LOW	129	0.1336	0.1312
na segment par	Current threshold TOO HIGH	58	0.2377	0.0724
na soma par	Current threshold TOO HIGH	58	-0.0510	0.7036
na node par	Current threshold TOO HIGH	58	-0.0451	0.7367
Km soma par	Current threshold TOO HIGH	58	0.3344	0.0103
Km axon par	Current threshold TOO HIGH	58	0.0752	0.5747
Kv soma par	Current threshold TOO HIGH	58	-0.1973	0.1377
Kv axon par	Current threshold TOO HIGH	58	-0.2381	0.0719
Kv1 soma par	Current threshold TOO HIGH	58	-0.0320	0.8116
Kv1 axon par	Current threshold TOO HIGH	58	0.0053	0.9683
na segment par	Input resistance TOO LOW	58	0.2440	0.0650
na soma par	Input resistance TOO LOW	58	-0.0779	0.5609
na node par	Input resistance TOO LOW	58	-0.0729	0.5868
Km soma par	Input resistance TOO LOW	58	0.3004	0.0219
Km axon par	Input resistance TOO LOW	58	0.0417	0.7562
Kv soma par	Input resistance TOO LOW	58	-0.1930	0.1467
Kv axon par	Input resistance TOO LOW	58	-0.1989	0.1344
Kv1 soma par	Input resistance TOO LOW	58	-0.0455	0.7347
Kv1 axon par	Input resistance TOO LOW	58	0.0386	0.7736
na segment par	Input resistance TOO HIGH	200	0.3091	0.0000
na soma par	Input resistance TOO HIGH	200	-0.0959	0.1769
na node par	Input resistance TOO HIGH	200	-0.0755	0.2882
Km soma par	Input resistance TOO HIGH	200	0.1204	0.0894
Km axon par	Input resistance TOO HIGH	200	-0.0155	0.8274
Kv soma par	Input resistance TOO HIGH	200	-0.4233	0.0000
Kv axon par	Input resistance TOO HIGH	200	0.2296	0.0011
Kv1 soma par	Input resistance TOO HIGH	200	0.0727	0.3062
Kv1 axon par	Input resistance TOO HIGH	200	0.1238	0.0807

Table A.1: Control Batch 1 fuzzy correlations.

Control Batch 2 Fuzzy Correlations				
parameter	objective fuzzy set	number of models	correlation coef	p value
na segment par	Current threshold TOO LOW	200	-0.0181	0.7990
na soma par	Current threshold TOO LOW	200	0.0427	0.5485
na node par	Current threshold TOO LOW	200	0.1190	0.0933
Km soma par	Current threshold TOO LOW	200	-0.2031	0.0039
Km axon par	Current threshold TOO LOW	200	-0.1755	0.0129
Kv soma par	Current threshold TOO LOW	200	-0.0310	0.6634
Kv axon par	Current threshold TOO LOW	200	-0.0287	0.6867
Kv1 soma par	Current threshold TOO LOW	200	0.1010	0.1548
Kv1 axon par	Current threshold TOO LOW	200	-0.1059	0.1355
na segment par	Current threshold TOO HIGH	241	-0.1147	0.0755
na soma par	Current threshold TOO HIGH	241	-0.1802	0.0050
na node par	Current threshold TOO HIGH	241	0.1665	0.0096
Km soma par	Current threshold TOO HIGH	241	0.1207	0.0613
Km axon par	Current threshold TOO HIGH	241	-0.1572	0.0145
Kv soma par	Current threshold TOO HIGH	241	-0.2390	0.0002
Kv axon par	Current threshold TOO HIGH	241	0.3438	0.0000
Kv1 soma par	Current threshold TOO HIGH	241	0.0588	0.3637
Kv1 axon par	Current threshold TOO HIGH	241	0.0184	0.7767
na segment par	Input resistance TOO LOW	241	-0.1278	0.0476
na soma par	Input resistance TOO LOW	241	-0.1676	0.0091
na node par	Input resistance TOO LOW	241	0.1747	0.0066
Km soma par	Input resistance TOO LOW	241	0.0846	0.1907
Km axon par	Input resistance TOO LOW	241	-0.1656	0.0100
Kv soma par	Input resistance TOO LOW	241	-0.2337	0.0003
Kv axon par	Input resistance TOO LOW	241	0.3439	0.0000
Kv1 soma par	Input resistance TOO LOW	241	0.0751	0.2452
Kv1 axon par	Input resistance TOO LOW	241	0.0207	0.7489
na segment par	Input resistance TOO HIGH	258	0.1232	0.0481
na soma par	Input resistance TOO HIGH	258	0.0558	0.3720
na node par	Input resistance TOO HIGH	258	-0.0280	0.6539
Km soma par	Input resistance TOO HIGH	258	-0.0421	0.5013
Km axon par	Input resistance TOO HIGH	258	-0.1005	0.1072
Kv soma par	Input resistance TOO HIGH	258	0.0844	0.1767
Kv axon par	Input resistance TOO HIGH	258	-0.1508	0.0153
Kv1 soma par	Input resistance TOO HIGH	258	-0.0893	0.1526
Kv1 axon par	Input resistance TOO HIGH	258	0.0103	0.8694

Table A.2: Control Batch 2 fuzzy correlations.

Control Batch 3 Fuzzy Correlations				
parameter	objective fuzzy set	number of models	correlation coef	p value
na segment par	Current threshold TOO LOW	92	0.3194	0.0019
na soma par	Current threshold TOO LOW	92	-0.2188	0.0362
na node par	Current threshold TOO LOW	92	-0.1246	0.2365
Km soma par	Current threshold TOO LOW	92	-0.1011	0.3376
Km axon par	Current threshold TOO LOW	92	-0.1127	0.2846
Kv soma par	Current threshold TOO LOW	92	0.1692	0.1068
Kv axon par	Current threshold TOO LOW	92	-0.0131	0.9011
Kv1 soma par	Current threshold TOO LOW	92	0.0378	0.7208
Kv1 axon par	Current threshold TOO LOW	92	0.0797	0.4501
na segment par	Current threshold TOO HIGH	231	-0.0198	0.7652
na soma par	Current threshold TOO HIGH	231	-0.2590	0.0001
na node par	Current threshold TOO HIGH	231	-0.0102	0.8771
Km soma par	Current threshold TOO HIGH	231	0.1601	0.0149
Km axon par	Current threshold TOO HIGH	231	-0.0498	0.4517
Kv soma par	Current threshold TOO HIGH	231	0.0066	0.9200
Kv axon par	Current threshold TOO HIGH	231	0.1341	0.0417
Kv1 soma par	Current threshold TOO HIGH	231	-0.0322	0.6265
Kv1 axon par	Current threshold TOO HIGH	231	-0.0759	0.2508
na segment par	Input resistance TOO LOW	231	-0.0370	0.5758
na soma par	Input resistance TOO LOW	231	-0.2232	0.0006
na node par	Input resistance TOO LOW	231	-0.0294	0.6562
Km soma par	Input resistance TOO LOW	231	0.1156	0.0797
Km axon par	Input resistance TOO LOW	231	-0.0552	0.4040
Kv soma par	Input resistance TOO LOW	231	0.0337	0.6106
Kv axon par	Input resistance TOO LOW	231	0.1502	0.0224
Kv1 soma par	Input resistance TOO LOW	231	-0.0355	0.5913
Kv1 axon par	Input resistance TOO LOW	231	-0.0657	0.3198
na segment par	Input resistance TOO HIGH	146	0.3122	0.0001
na soma par	Input resistance TOO HIGH	146	-0.0997	0.2312
na node par	Input resistance TOO HIGH	146	-0.0067	0.9364
Km soma par	Input resistance TOO HIGH	146	-0.2032	0.0139
Km axon par	Input resistance TOO HIGH	146	0.1168	0.1604
Kv soma par	Input resistance TOO HIGH	146	0.1131	0.1740
Kv axon par	Input resistance TOO HIGH	146	0.1066	0.2005
Kv1 soma par	Input resistance TOO HIGH	146	-0.0138	0.8682
Kv1 axon par	Input resistance TOO HIGH	146	-0.0130	0.8767

Table A.3: Control Batch 3 fuzzy correlations.

All Control Models Fuzzy Correlations				
parameter	objective fuzzy set	number of models	correlation coef	p value
na segment par	Current threshold TOO LOW	421	0.1563	0.0013
na soma par	Current threshold TOO LOW	421	-0.0266	0.5863
na node par	Current threshold TOO LOW	421	0.0553	0.2575
Km soma par	Current threshold TOO LOW	421	-0.0496	0.3101
Km axon par	Current threshold TOO LOW	421	-0.1461	0.0027
Kv soma par	Current threshold TOO LOW	421	0.0064	0.8955
Kv axon par	Current threshold TOO LOW	421	-0.0127	0.7947
Kv1 soma par	Current threshold TOO LOW	421	0.0847	0.0826
Kv1 axon par	Current threshold TOO LOW	421	0.0024	0.9608
na segment par	Current threshold TOO HIGH	530	0.0464	0.2862
na soma par	Current threshold TOO HIGH	530	-0.1906	0.0000
na node par	Current threshold TOO HIGH	530	0.0552	0.2045
Km soma par	Current threshold TOO HIGH	530	0.1395	0.0013
Km axon par	Current threshold TOO HIGH	530	-0.0049	0.9103
Kv soma par	Current threshold TOO HIGH	530	-0.1265	0.0035
Kv axon par	Current threshold TOO HIGH	530	0.1732	0.0001
Kv1 soma par	Current threshold TOO HIGH	530	-0.0086	0.8441
Kv1 axon par	Current threshold TOO HIGH	530	-0.0086	0.8433
na segment par	Input resistance TOO LOW	530	-0.0570	0.1900
na soma par	Input resistance TOO LOW	530	-0.1348	0.0019
na node par	Input resistance TOO LOW	530	0.0485	0.2654
Km soma par	Input resistance TOO LOW	530	0.0307	0.4813
Km axon par	Input resistance TOO LOW	530	-0.0795	0.0676
Kv soma par	Input resistance TOO LOW	530	-0.0803	0.0646
Kv axon par	Input resistance TOO LOW	530	0.2238	0.0000
Kv1 soma par	Input resistance TOO LOW	530	0.0173	0.6916
Kv1 axon par	Input resistance TOO LOW	530	-0.0163	0.7078
na segment par	Input resistance TOO HIGH	604	0.3818	0.0000
na soma par	Input resistance TOO HIGH	604	-0.0478	0.2411
na node par	Input resistance TOO HIGH	604	0.0573	0.1599
Km soma par	Input resistance TOO HIGH	604	0.2004	0.0000
Km axon par	Input resistance TOO HIGH	604	0.0720	0.0772
Kv soma par	Input resistance TOO HIGH	604	-0.2741	0.0000
Kv axon par	Input resistance TOO HIGH	604	-0.0867	0.0332
Kv1 soma par	Input resistance TOO HIGH	604	0.0209	0.6077
Kv1 axon par	Input resistance TOO HIGH	604	0.0536	0.1879

Table A.4: All Control models, fuzzy correlations.

Treated Batch 1 Fuzzy Correlations				
parameter	objective fuzzy set	number of models	correlation coef	p value
na segment par	Current threshold TOO LOW	162	0.2901	0.0002
na soma par	Current threshold TOO LOW	162	0.0356	0.6531
na node par	Current threshold TOO LOW	162	-0.0614	0.4380
Km soma par	Current threshold TOO LOW	162	-0.0627	0.4278
Km axon par	Current threshold TOO LOW	162	0.0306	0.6996
Kv soma par	Current threshold TOO LOW	162	0.1865	0.0175
Kv axon par	Current threshold TOO LOW	162	0.0540	0.4947
Kv1 soma par	Current threshold TOO LOW	162	-0.0589	0.4569
Kv1 axon par	Current threshold TOO LOW	162	-0.1474	0.0612
na segment par	Current threshold TOO HIGH	50	0.0232	0.8729
na soma par	Current threshold TOO HIGH	50	-0.3237	0.0219
na node par	Current threshold TOO HIGH	50	0.1994	0.1650
Km soma par	Current threshold TOO HIGH	50	-0.1653	0.2514
Km axon par	Current threshold TOO HIGH	50	0.0583	0.6875
Kv soma par	Current threshold TOO HIGH	50	0.0676	0.6408
Kv axon par	Current threshold TOO HIGH	50	-0.1394	0.3342
Kv1 soma par	Current threshold TOO HIGH	50	-0.2105	0.1423
Kv1 axon par	Current threshold TOO HIGH	50	-0.0141	0.9228
na segment par	Input resistance TOO LOW	123	0.2269	0.0116
na soma par	Input resistance TOO LOW	123	-0.2937	0.0010
na node par	Input resistance TOO LOW	123	0.0187	0.8375
Km soma par	Input resistance TOO LOW	123	0.1433	0.1139
Km axon par	Input resistance TOO LOW	123	-0.0933	0.3048
Kv soma par	Input resistance TOO LOW	123	-0.3023	0.0007
Kv axon par	Input resistance TOO LOW	123	0.1240	0.1718
Kv1 soma par	Input resistance TOO LOW	123	-0.2134	0.0178
Kv1 axon par	Input resistance TOO LOW	123	-0.1685	0.0624
na segment par	Input resistance TOO HIGH	130	0.1791	0.0414
na soma par	Input resistance TOO HIGH	130	-0.0870	0.3252
na node par	Input resistance TOO HIGH	130	0.0036	0.9680
Km soma par	Input resistance TOO HIGH	130	-0.1820	0.0382
Km axon par	Input resistance TOO HIGH	130	0.0439	0.6202
Kv soma par	Input resistance TOO HIGH	130	0.0657	0.4578
Kv axon par	Input resistance TOO HIGH	130	0.0566	0.5227
Kv1 soma par	Input resistance TOO HIGH	130	-0.0124	0.8890
Kv1 axon par	Input resistance TOO HIGH	130	0.0953	0.2809

Table A.5: Treated Batch 1 fuzzy correlations.

Treated Batch 2 Fuzzy Correlations				
parameter	objective fuzzy set	number of models	correlation coef	p value
na segment par	Current threshold TOO LOW	278	0.1351	0.0243
na soma par	Current threshold TOO LOW	278	0.0851	0.1571
na node par	Current threshold TOO LOW	278	-0.0028	0.9625
Km soma par	Current threshold TOO LOW	278	-0.3211	0.0000
Km axon par	Current threshold TOO LOW	278	0.0546	0.3641
Kv soma par	Current threshold TOO LOW	278	-0.0171	0.7764
Kv axon par	Current threshold TOO LOW	278	-0.1270	0.0342
Kv1 soma par	Current threshold TOO LOW	278	0.0190	0.7529
Kv1 axon par	Current threshold TOO LOW	278	0.0308	0.6093
na segment par	Current threshold TOO HIGH	143	-0.1833	0.0284
na soma par	Current threshold TOO HIGH	143	-0.2041	0.0145
na node par	Current threshold TOO HIGH	143	-0.0298	0.7242
Km soma par	Current threshold TOO HIGH	143	-0.0408	0.6281
Km axon par	Current threshold TOO HIGH	143	0.1508	0.0722
Kv soma par	Current threshold TOO HIGH	143	-0.1290	0.1246
Kv axon par	Current threshold TOO HIGH	143	0.0527	0.5317
Kv1 soma par	Current threshold TOO HIGH	143	-0.0257	0.7602
Kv1 axon par	Current threshold TOO HIGH	143	0.1912	0.0221
na segment par	Input resistance TOO LOW	197	-0.2002	0.0048
na soma par	Input resistance TOO LOW	197	-0.1622	0.0227
na node par	Input resistance TOO LOW	197	-0.0057	0.9362
Km soma par	Input resistance TOO LOW	197	-0.0913	0.2020
Km axon par	Input resistance TOO LOW	197	0.1914	0.0070
Kv soma par	Input resistance TOO LOW	197	-0.0125	0.8615
Kv axon par	Input resistance TOO LOW	197	0.1177	0.0995
Kv1 soma par	Input resistance TOO LOW	197	-0.0867	0.2259
Kv1 axon par	Input resistance TOO LOW	197	0.0089	0.9014
na segment par	Input resistance TOO HIGH	278	0.0971	0.1060
na soma par	Input resistance TOO HIGH	278	0.0820	0.1728
na node par	Input resistance TOO HIGH	278	0.0278	0.6448
Km soma par	Input resistance TOO HIGH	278	-0.2697	0.0000
Km axon par	Input resistance TOO HIGH	278	0.0652	0.2787
Kv soma par	Input resistance TOO HIGH	278	-0.0385	0.5225
Kv axon par	Input resistance TOO HIGH	278	-0.0975	0.1049
Kv1 soma par	Input resistance TOO HIGH	278	0.0015	0.9800
Kv1 axon par	Input resistance TOO HIGH	278	0.0007	0.9911

Table A.6: Treated Batch 2 fuzzy correlations.

Treated Batch 3 Fuzzy Correlations				
parameter	objective fuzzy set	number of models	correlation coef	p value
na segment par	Current threshold TOO LOW	69	0.3912	0.0009
na soma par	Current threshold TOO LOW	69	-0.2209	0.0682
na node par	Current threshold TOO LOW	69	-0.1481	0.2246
Km soma par	Current threshold TOO LOW	69	-0.3278	0.0060
Km axon par	Current threshold TOO LOW	69	-0.0606	0.6206
Kv soma par	Current threshold TOO LOW	69	0.1758	0.1486
Kv axon par	Current threshold TOO LOW	69	0.1801	0.1387
Kv1 soma par	Current threshold TOO LOW	69	0.0937	0.4436
Kv1 axon par	Current threshold TOO LOW	69	0.2642	0.0283
na segment par	Current threshold TOO HIGH	56	0.1180	0.3865
na soma par	Current threshold TOO HIGH	56	-0.5324	0.0000
na node par	Current threshold TOO HIGH	56	0.0416	0.7607
Km soma par	Current threshold TOO HIGH	56	-0.3135	0.0187
Km axon par	Current threshold TOO HIGH	56	0.0663	0.6273
Kv soma par	Current threshold TOO HIGH	56	-0.2101	0.1200
Kv axon par	Current threshold TOO HIGH	56	-0.0404	0.7673
Kv1 soma par	Current threshold TOO HIGH	56	-0.1653	0.2234
Kv1 axon par	Current threshold TOO HIGH	56	0.0446	0.7442
na segment par	Input resistance TOO LOW	99	0.0759	0.4551
na soma par	Input resistance TOO LOW	99	-0.3565	0.0003
na node par	Input resistance TOO LOW	99	0.0464	0.6483
Km soma par	Input resistance TOO LOW	99	0.0766	0.4511
Km axon par	Input resistance TOO LOW	99	-0.2177	0.0304
Kv soma par	Input resistance TOO LOW	99	-0.1714	0.0898
Kv axon par	Input resistance TOO LOW	99	-0.2093	0.0376
Kv1 soma par	Input resistance TOO LOW	99	-0.1088	0.2836
Kv1 axon par	Input resistance TOO LOW	99	0.0270	0.7910
na segment par	Input resistance TOO HIGH	69	0.3376	0.0046
na soma par	Input resistance TOO HIGH	69	-0.1797	0.1396
na node par	Input resistance TOO HIGH	69	-0.1102	0.3675
Km soma par	Input resistance TOO HIGH	69	-0.2933	0.0144
Km axon par	Input resistance TOO HIGH	69	-0.0487	0.6911
Kv soma par	Input resistance TOO HIGH	69	0.2031	0.0942
Kv axon par	Input resistance TOO HIGH	69	0.1886	0.1207
Kv1 soma par	Input resistance TOO HIGH	69	0.0549	0.6539
Kv1 axon par	Input resistance TOO HIGH	69	0.2031	0.0941

Table A.7: Treated Batch 3 fuzzy correlations.

All Treated Models Fuzzy Correlations				
parameter	objective fuzzy set	number of models	correlation coef	p value
na segment par	Current threshold TOO LOW	509	0.1808	0.0000
na soma par	Current threshold TOO LOW	509	0.0265	0.5511
na node par	Current threshold TOO LOW	509	-0.0458	0.3025
Km soma par	Current threshold TOO LOW	509	-0.1686	0.0001
Km axon par	Current threshold TOO LOW	509	0.0288	0.5172
Kv soma par	Current threshold TOO LOW	509	0.0529	0.2339
Kv axon par	Current threshold TOO LOW	509	-0.0179	0.6873
Kv1 soma par	Current threshold TOO LOW	509	-0.0019	0.9663
Kv1 axon par	Current threshold TOO LOW	509	0.0012	0.9783
na segment par	Current threshold TOO HIGH	249	-0.0976	0.1244
na soma par	Current threshold TOO HIGH	249	-0.2313	0.0002
na node par	Current threshold TOO HIGH	249	0.0414	0.5153
Km soma par	Current threshold TOO HIGH	249	-0.1765	0.0052
Km axon par	Current threshold TOO HIGH	249	0.0962	0.1299
Kv soma par	Current threshold TOO HIGH	249	-0.1217	0.0551
Kv axon par	Current threshold TOO HIGH	249	-0.0498	0.4339
Kv1 soma par	Current threshold TOO HIGH	249	-0.0835	0.1892
Kv1 axon par	Current threshold TOO HIGH	249	0.1434	0.0236
na segment par	Input resistance TOO LOW	419	0.1510	0.0019
na soma par	Input resistance TOO LOW	419	-0.2706	0.0000
na node par	Input resistance TOO LOW	419	-0.0085	0.8626
Km soma par	Input resistance TOO LOW	419	0.1485	0.0023
Km axon par	Input resistance TOO LOW	419	0.0284	0.5617
Kv soma par	Input resistance TOO LOW	419	-0.0595	0.2238
Kv axon par	Input resistance TOO LOW	419	0.1112	0.0229
Kv1 soma par	Input resistance TOO LOW	419	-0.1208	0.0133
Kv1 axon par	Input resistance TOO LOW	419	-0.0408	0.4049
na segment par	Input resistance TOO HIGH	477	0.0777	0.0900
na soma par	Input resistance TOO HIGH	477	0.0082	0.8576
na node par	Input resistance TOO HIGH	477	0.0019	0.9675
Km soma par	Input resistance TOO HIGH	477	-0.2382	0.0000
Km axon par	Input resistance TOO HIGH	477	0.0474	0.3016
Kv soma par	Input resistance TOO HIGH	477	0.0032	0.9452
Kv axon par	Input resistance TOO HIGH	477	-0.0229	0.6175
Kv1 soma par	Input resistance TOO HIGH	477	0.0133	0.7728
Kv1 axon par	Input resistance TOO HIGH	477	0.0522	0.2551

Table A.8: All Treated models, fuzzy correlations.